INVESTIGATING THE EFFECT OF ACTIVATING AGENTS ON REMOVAL OF LEAD IONS FROM WATER USING ACTIVATED RICE HUSK CARBON

BY

IVAN KAMUKAMA

(BEng. Civil and Building Engineering, KYU)

22/U/GMEW/259/PE

A DISSERTATION SUBMITTED TO THE DIRECTORATE OF RESEARCH AND GRADUATE TRAINING OF KYAMBOGO UNIVERSITY IN PARTIAL FULFILMENT OF THE REQUIREMENTS FOR THE AWARD OF MASTER OF SCIENCE IN WATER AND SANITATION ENGINEERING DEGREE OF KYAMBOGO UNIVERSITY

SEPTEMBER, 2025

DECLARATION

I Ivan Kamukama, hereby declare that this submission is my own work and that, to the best of my knowledge and belief, it contains no material previously published or written by another person nor material that has been accepted for the award of any other degree of the university or other institute of higher learning, except where due acknowledgment has been made in the text and reference list.

Signed: ……..…….. Date: …….

APPROVAL

The undersigned approves that he has read and hereby recommends for submission to the Directorate of Research and Graduate Training of Kyambogo University, a dissertation titled “Investigating the effect of activating agents on removal of lead ions from water using activated rice husk carbon” in fulfilment of the requirements for the award of Master of Science in Water and Sanitation Engineering Degree of Kyambogo University.

Dr. Charles Onyutha

Signed: ……..……. Date: ……

ACKNOWLEDGEMENTS

I want to convey my thanks to God for guiding me this far, particularly in maintaining good health and achieving success in my academic pursuits.

I am sincerely thankful to my esteemed supervisor, Dr. Charles Onyutha, for the unwavering encouragement, guidance, and invaluable advice throughout the entirety of this research. His suggestions, comments, and timely corrections after thoroughly reviewing my work have been greatly appreciated.

I would also like to acknowledge the lecturers and staff of the Department of Civil and Environmental Engineering at Kyambogo University for their substantial assistance during the course of this study.

Furthermore, I am indebted to coworkers and fellow students for their helpful concepts and guidance that they provided throughout my academic journey.

Lastly, I am sincerely thankful to my family and friends for their constant backing, motivation, tolerance, and comprehension while I was not present.

TABLE OF CONTENTS

LIST OF TABLES

LIST OF FIGURES

LIST OF ACRONYMS

ARHC : Activated Rice Husk Carbon

ARHCK : Activated Rice Husk Carbon treated with Potassium Hydroxide

ARHCZ : Activated Rice Husk Carbon treated with Zinc Chloride

ARHCH : Activated Rice Husk Carbon treated with Phosphoric Acid

ICP-OES : Inductively Coupled Plasma-Optical Emission Spectroscopy

RHC : Rice Husk Carbon

SEM : Scanning Electron Microscope

WHO : World Health Organisation

UN : United Nations

UNICEF : United Nations Children's Fund

LIST OF SYMBOLS

% : Percent

Pb^{2+} ions : Lead (II) ions

KOH : Potassium Hydroxide

$ZnCl_2$: Zinc Chloride

H_3PO_4 : Phosphoric Acid

H_2SO_4 : Sulfuric acid

L : Liter

g : grams

mL : Milliliters

mg : Milligrams

g/L : grams per liter

mg/L : Milligram per liter

^oC : Degrees Celsius

$Pb(NO_3)_2$: Lead (II) nitrate

ppm : Parts per million

mol : Mole

LIST OF ABBREVIATIONS

etc : etcetera

e.g : For example

min : Minutes

hr : Hour

Sec : Second

max : Maximum

ABSTRACT

Activated carbon is very important in treating polluted water. Carbon can be produced from locally sourced agricultural waste. This helps in reducing the amount of agricultural waste in the environment. This study investigated the effect of activating agents on removal of Pb^{2+} ions from water using activated rice husk carbon. Chemical activation method was used where rice husk carbon (RHC) was impregnated with chemical activating agents before heating. Three distinct activating agents were used namely; potassium hydroxide (KOH), phosphoric acid (H_3PO_4) and zinc chloride ($ZnCl_2$). RHC activated with a 7.5% concentration of KOH using 5g/L adsorbent showed 99.9% efficiency in removing lead ions, almost achieving complete elimination. RHC activated with 1% $ZnCl_2$ while using 20g/L adsorbent demonstrated 98.5% removal efficiency, just 1.36% less than the RHC activated with 7.5% KOH. RHC activated with 2.5% H_3PO_4 while using 20g/L adsorbent showed 84.1% removal efficiency, making it least effective among the three agents tested at their optimal levels. Despite achieving removal efficiencies of 98.5% and 84.1%, RHC activated with $ZnCl_2$ and H_3PO_4, respectively, required a higher adsorbent dosage (20 g/L), indicating lower effectiveness compared to KOH-activated carbon. KOH activation created a highly porous and rough surface with a well-developed network of interconnected pores. On the other hand, $ZnCl_2$ and H_3PO_4 resulted in less aggressive pore formation and different surface morphologies, leading to less interconnected and less rough porous structures. It was observed that the uptake of Pb^{2+} ions by activated RHC aligns more accurately with the Langmuir isotherm model.

Keywords: Activated carbon, rice husk, activating agents, Pb^{2+} ions

CHAPTER ONE: INTRODUCTION

1.1 Background of the study

The worldwide rise in industrialisation and agrochemicals has led to an increase in toxic pollutions in the environment causing a growing scarcity of clean water (Van Vliet et al., 2021). Unfortunately, many industries and human-related activities lead to discharges of sewage and waste water that has not undergone treatment directly into the aquatic systems and across the terrestrial environments (Dietler et al., 2019). In Uganda especially in urban centers with industrial effluents, such as Kampala, Mukono, Jinja, elevated levels of heavy metals, particularly lead, have been detected in water sources (Baguma et al., 2022). Lead (II) ions (Pb^{2+} ions) is a common water pollutant. Through various food chains and water consumption, toxic pollutants gradually build up in human tissues leading to the onset of different illnesses like failure of the kidneys, liver, brain, reproductive organs, and nervous system, and in severe cases, resulting in death. The provisional limit for Pb^{2+} ions in potable water should not exceed 10 µg/L, and intervention is recommended when blood Pb^{2+} ions levels are equal to or exceed 5 µg/dL (WHO, 2023). Additionally, significant contact with lead (II) ions has been associated with infertility, miscarriages and deaths of newborns shortly after birth (Parthasarathy and Narayanan, 2014).

Various conventional physicochemical water purification techniques like membrane filtration, oxidation/reduction, adsorption, ion exchange and chemical precipitation have been utilised for some time to remove toxic pollutants (Singh et al., 2017). Adsorption has gained worldwide recognition as the preferred option endorsed by environmentalists, owing to its cost-effectiveness, superior performance, versatility,

and safe handling without the production of any toxic intermediates or byproducts (Kim et al., 2019). Several agricultural by-products, including rice husk which are abundantly available at minimal or no cost, have been found to possess the ability to effectively eliminate significant quantities of metal ions and organic contaminants from solutions that are water-based (Sharifikolouei et al., 2020). The use of agricultural byproducts like rice husk addresses waste management challenges while simultaneously offering a renewable and a cost-effective method for producing activated carbon. This approach promotes environmental conservation and resource recovery efficiency (Tamer et al., 2013). Additionally, Uganda generates large quantities of rice husk as an agricultural waste, particularly in areas like Kibuku, Lira, Iganga, and Hoima, which remain underutilized. Therefore, exploring the capability of locally available rice husk as a low-cost precursor for activated carbon offers a sustainable solution for improving access to safe drinking water.

Activated carbon, commonly referred to as activated charcoal or coal, belongs to the category of carbonaceous materials that undergoes processing to create an exceedingly microporous network possessing a substantial surface area, facilitating its effectiveness in adsorption or chemical reactions (Sevilla et at., 2021). In both environmental and industrial fields, activated carbon serves as a key material for the removal of organic pollutants in wastewater treatment, treatment of industrial effluents and, air and gas purification but its major application is in water treatment (Jiang et al., 2019). Activated carbon is derived from agricultural and forest waste such as coal, wood, rice husk, coconut shell, and other biomass through an activation process. These wastes have demonstrated great promise as suitable percussor materials and this is primarily

attributed to their widespread accessibility at an affordable price (Canales-Flores and Prieto-García, 2016).

An essential factor in assessing the efficiency and suitability of activated carbon depends on the choice of a suitable activating agent, which plays a pivotal role in controlling its performance and applicability (Oribayo et al., 2020). Activating agents are categorized as basic, neutral, acidic, or self-activating. They interact with biomass components to influence activation. Common agents include phosphoric acid (H_3PO_4), zinc chloride ($ZnCl_2$), potassium hydroxide (KOH), sodium hydroxide (NaOH), sodium bicarbonate ($NaHCO_3$), and sulfuric acid (H_2SO_4) (Gao et al., 2020). KOH results in excellent performance for microporous carbon but costly and corrosive, $ZnCl_2$ results in good porosity but declining use due to toxicity and environmental impact, H_3PO_4 produces high surface area but slightly less effective for creating microporous structure than KOH (Din et al., 2017). The primary objective of the activation process is to enhance pore volume, enlarge pore diameter, and improve the overall porosity of activated carbon. This can be accomplished through three separate approaches: physical activation, chemical activation, and a combination of both processes, known as physicochemical activation (Canales-Flores and Prieto-García, 2016).

Research has explored the elimination of Pb^{2+} ions from water using natural materials in raw form (Kumar, 2014) and in activated forms (Thitame and Shukla, 2017) and the performance of the two forms of adsorbents has been different. However, there is limited comprehensive analysis on the specific impact of different activating agents on Pb^{2+} ions removal from water. Therefore, this knowledge is important in improving the efficiency of removal of Pb^{2+} ions from water. Efficient and affordable extraction of

trace metals from water is vital for increasing a global supply of safe water and improving human health. Implementing cost-effective techniques for removing toxic pollutants from drinking water benefits water treatment companies and households especially in developing countries where safe water is scarce.

This work concentrated on investigating the capability of activated rice husk carbon (ARHC) in eliminating harmful heavy metals specifically Pb^{2+} ions from water. This investigation sought to provide information to guide water managers regarding the choice of activating agent in optimisation of adsorption of Pb^{2+} ions from water.

1.2 Problem statement

The increasing industrialisation and use of agrochemicals has led to the emission of harmful pollutants, primarily containing toxic metal ions (Azimi et al., 2017). Many locations in the world have surface water sources with heavy metal levels surpassing permissible limits for drinking water (Chowdhury et al., 2022). A range of techniques has been established to extract heavy metals from water. However, the conventional treatments come with limitations, such as incomplete removal, formation of toxic residue, cost and technical constraints leading to inadequate implementation of these technologies, thus posing a significant global challenge (Singh et at., 2017). Lead is a highly hazardous heavy metal frequently detected in contaminated water sources, and its accumulation in the human body can cause severe health problems, including damage to the brain, kidneys, and reproductive system (Rehman et al., 2018). Despite the proven efficiency of activated carbon in eliminating toxic metals from water, the effectiveness of this method significantly depends on the activating agent used during the preparation process (Youssef et al., 2015). While rice husk is a promising low-cost

precursor for producing activated carbon (Sharifikolouei et al., 2020), there has been a dearth of information on how different activating agents influence its performance in removing Pb^{2+} ions from water. This research aimed to fill this gap by examining the impact of various activating agents on the efficiency of rice husk-based activated carbon in Pb^{2+} ions removal from water, thereby contributing to efforts aimed at providing safe drinking water and protecting public health.

1.3 Main and specific objectives

1.3.1 Main objective

The main objective was to investigate the effect of activating agents on removal of lead ions from water using activated rice husk carbon, with specific focus on providing low-cost water purification solutions for urban communities in Uganda.

1.3.2 Specific objectives

The specific objectives were:

i) To optimise the concentration of the activating agents.

ii) To characterise the surface structure of the RHC when it is both activated and not activated.

iii) To examine the adsorption of lead ions using rice husk carbon activated using various activating agents.

1.4 Research questions

i) What is the optimal concentration of activating agents for maximising adsorption of Pb^{2+} ions from water?

ii) How does the surface structure of the Rice Husk Carbon differ between its activated and non-activated states?

iii) How does the adsorption of Pb^{2+} ions vary when using Rice Husk carbon activated with different activating agents?

1.5 Significance of the study

The study provides a better insight into the removal of Pb^{2+} ions from water using ARHC, supporting both locals and professionals in creating effective water treatment solutions. It presents an affordable, environmentally conscious and sustainable strategy for eliminating Pb^{2+} ions from water thus, improving existing water treatment processes or developing new Pb^{2+} ion removal technologies. Additionally, the study sheds light on potential value and sustainable usage of rice husk as a material for creating activated carbon, stimulating the development of innovative waste management methods and opening up new opportunities for utilising agricultural by-products. Finally, because Pb^{2+} ions contamination in drinking water poses substantial health hazards, this research helps to create safe and effective water treatment method resulting in greater access to clean and Pb^{2+} ions-free drinking water, hence, improving public health and well-being of the general public. The results contribute directly to the realization of SDG 6 - ensuring sustainable water availability and management and SDG 3, which is centered on safeguarding healthy lives and fostering well-being across all age groups.

1.6 Research scope

1.6.1 Time scope

The duration of research was 13 months starting from July 2023 up to the end of July 2024.

1.6.2 Geographical scope

The research was conducted from the chemistry laboratory under chemistry department, faculty of science of Kyambogo university, and Materials laboratory under the College of Engineering, Design, Art and Technology of Makerere university, found in Kampala city-Uganda.

1.6.3 Content scope

i) The research used three activating agents including phosphoric acid (H_3PO_4), zinc chloride ($ZnCl_2$) and potassium hydroxide (KOH).

ii) The research was limited to removal of Pb^{2+} ions.

iii) The carbon was in the form of rice husk.

1.7 Conceptual framework

The main independent and dependent variables were activating agents and Pb^{2+} ions removal from water, respectively. The intervening variables included factors such as pH, temperature and the selected genotype of the rice.

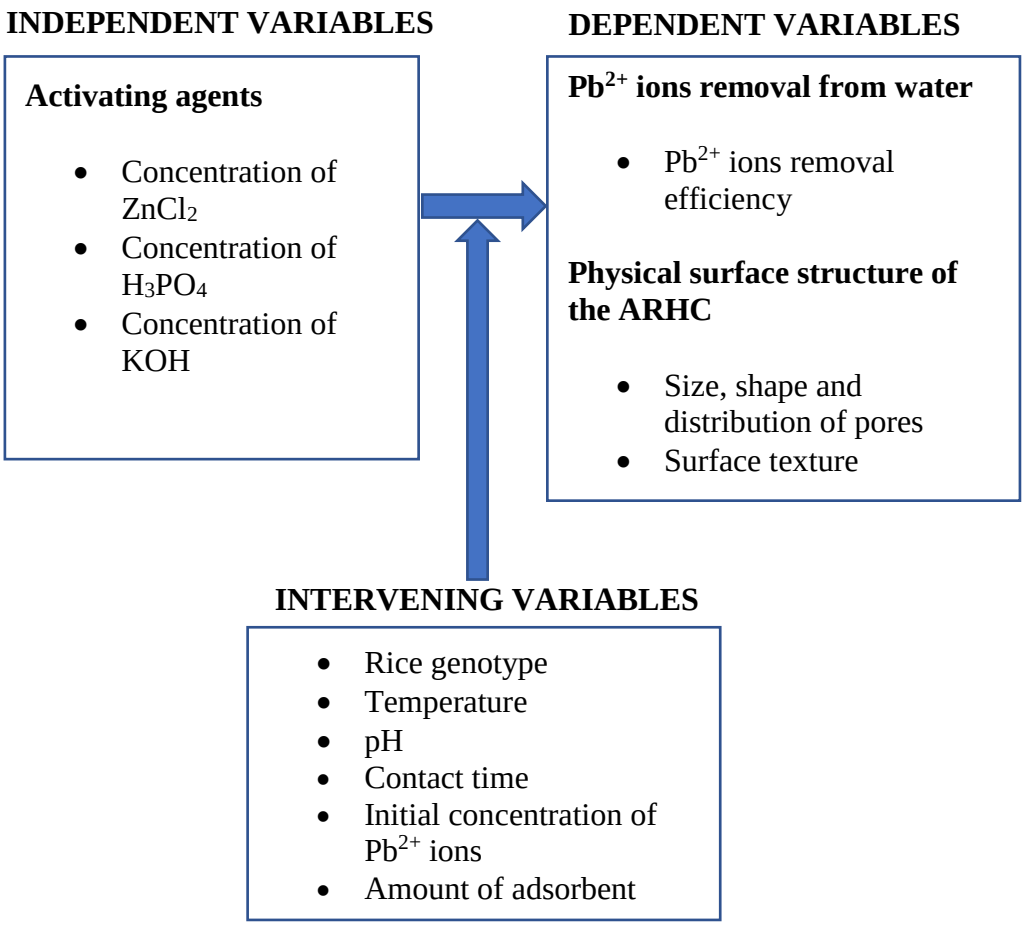

Figure 1.1: Conceptual framework

1.8 Chapter summary

Water scarcity is the alarming condition posing significant challenges to communities and ecosystems worldwide. Water scarcity is occasionally linked to low water quality, particularly the existence of trace metals. The presence of high concentrations of toxic metals in water creates significant health risks to humans. Activated carbon produced from rice husk is known for its potential in adsorbing substances from solution. Several studies have indicated that the type of activating agent can affect adsorption of adsorbents. It holds significance to determine how the type of activating agent affects removal of Pb^{2+} ions from water using ARHC. This research could contribute to the

development of affordable and environmentally friendly water treatment methods for the removal of Pb^{2+} ions from polluted water sources. In summary, this chapter identified the issue at hand and presented clear objectives aimed at addressing several research inquiries.

CHAPTER TWO: LITERATURE REVIEW

2.1 Scarcity of clean water

The levels of water scarcity and the proportion of individuals facing severe water scarcity are significantly greater when considering both water quality (averaging 40%) and water quantity (30%) rather than focusing solely on water quantity (Van Vliet et al., 2021). Uganda experiences inequalities in water access resulting from the geographical distribution of water points and population densities (Kamya et al., 2020). Poor water quality results from deficient waste management, system neglect, flooding, urban planning issues, inadequate treatment, population growth, political interference and water hyacinth spread (Id et al., 2023).

2.2 Water contamination by lead

Heavy metals are constantly discharged into aquatic environments from diverse natural and human-induced sources (Zamora-Ledezma et al., 2021). Trace metal ions pose a significant issue because of their prevalence as released contaminants, making them troubling (Azimi et al., 2017). Existence of trace metals in water can endanger both human well-being and the environment. Lead is among the harmful heavy metals that have the potential to create hazards when people come into contact with them through water and air environments (Wani et al., 2015).

Inadequate removal of trace metals during water treatment may result in their accumulation in the human body and the environment, causing health problems and environmental degradation. Heavy metals such as lead can accumulate in human body organs like the brain, liver, heart and kidneys and interrupt regular biological processes

(Rehman et al., 2018). Moreover, they are linked to infertility, miscarriages, stillbirths, and neonatal mortality and sometimes death (Sharma et al., 2023). Report of the World Health Organization's 10^{th} International Lead Poisoning Prevention Week (ILPPW) that took place on 23-29 October 2022 showed that approximately 1 million people lose their lives annually as a result of lead poisoning, leading to a higher number of children experiencing lasting health consequences. United Nations International Children's Emergency Fund estimates that as many as 800 million children worldwide, which is equivalent to one out of every three children have blood lead levels meeting or exceeding 5 µg/dL.

Lead has the potential to impact nearly all bodily organs and systems in humans. Even minimal quantities of lead in the bloodstream of children may result in issues like hearing and learning difficulties, anemia,, stunted growth, reduced intelligence quotient, and increased hyperactivity (Wani et al., 2015). An immediate intervention is recommended when blood Pb^{2+} ion levels reach or surpass 5 µg/dL (WHO, 2023). Furthermore, grown-ups who come into contact with lead may experience cardiovascular issues, elevated blood pressure, higher occurrence of hypertension, reduced kidney functionality, premature birth and challenges related to reproduction (Rehman et al., 2018).

2.3 Activated carbon

Activated carbon comprises a collection of substances characterised by extensively enhanced porous nature and a large surface area between particles that finds increasing use in the purification of water and wastewater, purification of air and desalination (Heidarinejad et al., 2020). Activated carbons are widely recognised carbonaceous

materials that possess numerous open or easily accessible micro-pores and meso-pores within their structure; the traditional terminology used for activated carbon is ‘activated charcoal’ (Lee et al., 2014). Any carbon-rich substance can be used to produce activated carbon with varying properties depending on the raw material, the type of activating agent used, and the specific conditions applied during the preparation process (Kosheleva et al., 2019).

2.3.1 Raw materials

An economical substance rich in carbon and possessing minimal inorganic components, specifically a low ash content, is the favored choice as the primary material for manufacturing activated carbon (Elsayed and Zalat, 2015). Over the past 20 years, industrial and agricultural waste materials have garnered interest for their ready availability, cost-effectiveness, minimal environmental harm, and their dual use as both adsorbents and raw materials for producing activated carbon (Abbas et al., 2020). Agricultural wastes like sugar cane bagasse, plant straws, nut shells, seed husks, and agro-forestry residues are valuable resources that can be utilised as alternative materials for producing activated carbon (Heidarinejad et al., 2020). Various factors, including raw material properties, pretreatment process, activation degree, and method, influence the adsorptive properties of activated carbon (Menya et al., 2018). Rice husk, a type of lignocellulosic biomass composed of hemicellulose, lignin and cellulose possesses physical and biochemical characteristics that render it suitable for producing activated carbon (Olupot et al., 2016).

2.3.2 Activating agents

Activating agents for carbon can mainly be categorised into 4 groups: basic, neutral, acidic and self-activating agents. Depending on the type, these activating chemicals interact with hemicellulose, cellulose, lignin, or polysaccharide present in the carbon precursor, resulting in diverse processes of activation (Gao et al., 2020b). Commonly used reagents for activating carbon from agricultural materials include phosphoric acid, zinc chloride, potassium hydroxide, sodium hydroxide, sodium bicarbonate and sulfuric acid (Alam et al., 2020). Basic activation treatment such as the use of potassium hydroxide provides a better yield but is slightly expensive, neutral treatment for instance in terms of zinc chloride is safe but yields less amount of activated carbon making it economically unfavorable (Din et al., 2017). Therefore, acidic treatment like using phosphoric acid is the best treatment, offering better surface area and micro-porosity when carefully controlled (Din et al., 2017). This study aims to investigate the utilisation of potassium hydroxide, zinc chloride and phosphoric acid as activating agents for the rice husk-based carbon.

2.4 Production of activated carbon

Activated carbon is produced by applying two main processes including carbonisation and activation (Yue and Economy, 2017). It can be generated by mixing the carbon rich material with chemical agent solution, then the mixture pyrolyed in a reactor with a fixed bed made of stainless steel and gradually heated at 7^{o}C/min until it attained 700^{o}C (Korobochkin et al., 2016). Since rice husk possesses an elevated level of silica composition, leaching with alkali hydroxide is a preferred technique to produce activated carbon and in this process, the rice husks are first carbonised at 500^{o}C for 90

minutes in an environment rich in nitrogen gas followed by impregnation with activating agents (Van et al., 2019).

2.4.1 Carbonisation

Carbonisation process involves increasing the carbon concentration in carbon-based substances by removing non-carbon elements through the use of heat-induced decomposition (Mohamad-Nor et al., 2013). During carbonisation, it is necessary to expose the material to a certain level of heat below 700^{o}C in distillation apparatus; this temperature enables the evaporation and elimination of hydrocarbons from the material in an oxygen-free environment (Heidarinejad et al., 2020). Generally, the carbonisation procedure can be described as a pyrolytic process, resulting in the formation of carbonised substance, which is commonly referred to as char or bio-char (Byamba-Ochir et al., 2016). Korobochkin et al. (2016) conducted carbonisation process on rice husks at an optimal temperature (850^{o}C) resulting in substance comprising 43.3% carbon and 25.9% silica by weight.

2.4.2 Activation

Activation of carbon is the process of improving the adsorptive properties of carbon materials by creating high porosity, achieved through specific chemical or physical treatments (Heidarinejad et al., 2020). The process of carbon activation entails subjecting the carbon material to temperature (400^{o}C - 900^{o}C) exposed to air, carbon dioxide, or steam (Vilén et al., 2022).

Chemical activation

Chemical activation entails soaking raw materials with different kinds of chemicals and subjecting them to high-temperature 500^{o}C - 1000^{o}C in the presence of an enclosed atmosphere or unreactive gases (Alam et al., 2020). The chemical activation method combines carbonisation and activation into one step, allowing both processes to occur simultaneously and this is achieved by mixing a precursor material with chemical activating agents that work as drying agents and substances that promote oxidation (Ahmad et al., 2013). When contrasted with physical activation, chemical activation methods result in porous carbons with enhanced pore formation (pore volumes exceeding 1 cm^3g^{-1} and Brunauer-Emmett-Teller surface areas surpassing 2000 m^2g^{-1}), as well as a pore structure that typically merges both micro and mesopores (Sevilla et al., 2021). Kane et al. (2016) impregnated 20 grams of carbon derived from rice husk with H_3PO_4 and KOH solutions of different concentrations at room temperature for 1.5 hours during the process of activation. The findings indicated that H_3PO_4 is slightly more effective than KOH in producing activated carbon for sodium lauryl sulfate adsorption, likely due to its greater ability to open the carbon structure. Rice husk-derived activated carbon exhibits high adsorption capacity for sodium lauryl sulfate when activated with H_3PO_4 at a temperature of 450^{o}C. This is because H_3PO_4 removes carbonization impurities and enhances pore development by forming phosphate bonds that connect biopolymer fragments and increase surface area (Kane et al., 2016). Activation temperature varies from 400^{o}C to 900^{o}C based on the activating agent and the intended final product characteristics, causing cellulose degradation during the process (Heidarinejad et al., 2020).

2.5 Conditions for preparation of activated carbon

Major conditions that affect production of activated carbon include carbon-rich unprocessed material, activating agent, activating temperature and time, concentration of activating agent, raw material: activating agent impregnation ratio (Menya et al., 2018).

2.5.1 Concentration of activating agent

Michuki (2015) found out that the elimination percentage of Pb^{2+} ions exhibited a gradual rise, moving from 62.6% to 85.2%, as the acid concentration for activating the carbon changed from 10% to 50%. The capacity of activated carbon to capture and to retain Pb^{2+} ions changes very little as the concentration of activating agents like H_3PO_4 and KOH is raised (Kane et al., 2016).

2.5.2 Impregnation ratio

Korobochkin et al. (2016) mixed 150 g of air-dried biomass with varying concentrations of activating agent solution at soaking ratios of 1:1, 1:2, 1:3 and 1:4 (mass of biomass to be soaked / activating agent weight), the yield of activated carbon obtained from rice husk increased proportionally with the amount of activating agent applied. Activation at optimal impregnation ratio gives maximum adsorption capacity i.e. 1:4 (weight of RHC to weight of KOH) (Guo et al., 2002), 1:5 for H_3PO_4 treated activated carbon (Li et al., 2011) and 1:2 for $ZnCl_2$ treated activated carbon (Liou and Wu, 2009)

2.5.3 Activating temperature and time

Typically, the ideal activation temperature for acidic activating agents falls within the 400–500°C range, while alkaline and self-activating agents generally show optimal activation temperatures in the 750–850°C range (Redondo et al., 2015). The rice husk carbonised at 800^{o}C gives an enhanced adsorption ability for Nickle, Zinc and lead ions than the ones carbonised at 400^{o}C and 600^{o}C (Gao et al., 2020b). The optimum activating temperature and time is 500^{o}C and 30 minutes, respectively for H_3PO_4 (Li et al., 2011), that of KOH is 800^{o}C for 1 hour (Guo et al., 2002) while that of $ZnCl_2$ is 500^{o}C for 1 hr and 40 minutes (Latiff et al., 2016).

2.6 Conventional approaches for extracting lead from water

Due to recognised harmful impacts of lead, several methods have been created for the purpose of eliminating these ions from waste releases. Some of the common approaches for eliminating lead from water are precipitation, membrane filtration, ion exchange, coagulation-flocculation and adsorption (Arbabi and Hemati, 2015).

2.6.1 Chemical precipitation

Chemical precipitation involves introducing a suitable solution into water containing Pb^{2+} ions, which results in pH elevation. Consequently, a portion of the dissolved lead is prompted to form a solid precipitate. This solid lead compound can later be eliminated by either allowing it to settle through sedimentation or by using a filtration procedure (Sadeghi et al., 2017).

2.6.2 Ion exchange

Lead ions possess a positive electrical charge; an ionic exchange procedure uses this characteristic to trap the pollutant. Water flows across a polymer resin embedded with anionic chemical units whereby these negatively charged ions attach to the lead. Following this process, lead concentrations in the water frequently decrease to a point suitable for safe release (Lalmi et al., 2018).

2.6.3 Membrane filtration

Under pressure, water is forced through membranes featuring carefully engineered pores. These minuscule apertures prevent lead ions from passing and redirect them into a distinct flow. By passing water through a sequence of these membranes, the lead concentration is reduced to permissible levels, all without introducing additional chemicals into the water flow (Efome et al., 2019).

2.6.4 Adsorption

During the course of adsorption, water passes through a material selected for its capacity to extract lead ions. Activated charcoal and biomass offer efficient methods for removing ionic lead from a solution. In the majority of industrial settings, adsorption presents a cost-effective choice for treating water. However, industries with manufacturing operations generating substantial lead concentrations might encounter challenges due to the need for frequent media replacement, which can prove to be both inconvenient and costly (Yarkandi, 2014).

Among the techniques for removal of metal ions, the selection of adsorption is based on its appropriateness as the preferred method due to its affordability, user-friendliness,

exceptional effectiveness in lead removal and the use of readily available and easily disposable materials (Zamora-Ledezma et al., 2021; Chowdhury et al., 2022).

2.7 Pb^{2+} ions removal from water using ARHC

In the past two decades, rice husks have gained attention for their potential use as a substance for extracting lead and trace metals from polluted water due to their abundance and low toxicity. They are utilised as adsorption agents, either in their natural form or after activation with acids or bases, resulting in the advancement of substances like activated carbon, activated charcoal, and silica. The use of rice husks is exceptionally effective in purifying lead-contaminated water, with lead ion removal rates ranging from 75% to 99% in liquid solutions (Abbas et al., 2020).

2.7.1 Past studies on chemical activation of rice husk carbon

Khashan and Mohammad (2022) conducted a lab-scale investigation to assess the potential of utilizing rice husk-derived activated carbon for the removal of Pb^{2+} ions from simulated wastewater. They compared three forms of rice husks: natural (untreated), activated with H_2SO_4 and activated with KOH. The study aimed to determine which form of activated carbon was most effective in removing Pb^{2+} ions. After carbonization, the husks were chemically activated using either H_2SO_4 or KOH, with the activated carbon being produced at 650°C for 2 hours and 20 minutes under nitrogen flow. The maximum efficiency achieved in Pb^{2+} ion removal was 97.25% for KOH-activated carbon, 92.3% for H_2SO_4-activated carbon, and 51.21% for natural rice husks. The study concluded that activated rice husk carbon, especially when activated with KOH, is a highly effective adsorbent for removing Pb^{2+} ions from wastewater. The

authors recommended exploring other activation methods and conditions to optimize elimination of various heavy metals through adsorption.

Aroh and Aroh (2022) examined the effect of various activating agents on the properties of activated carbon obtained from carbon rods in spent batteries. Five different chemical activating agents were used (i.e., Sodium Hydroxide, Sodium Carbonate, KOH, Potassium Carbonate, and $ZnCl_2$) to understand their influence on various characteristics of activated carbon such as density, volatile components, carbonaceous content, ash content, and moisture level. The study concluded that the selection of activating agent significantly influences the characteristics of activated carbon. These properties include density, percentage ash content, moisture content, volatile matter, surface structure and organic carbon. Potassium hydroxide was found to be the most efficient for generating activated carbon with enhanced organic carbon content.

Babatunde and Ibrahim (2020) investigated the removal of heavy metals via adsorption, specifically lead (Pb) and cadmium (Cd), from wastewater using activated rice husk carbon (ARHC) and inactivated RHC. The objective of the research was to determine the adsorption capacities of ARHC and inactivated RHC for removing these metals and to assess the effect of different factors such as adsorbent dosage, pH, concentration of metal ion, and contact time on the process of adsorption. ARHC was prepared by soaking rice husk in ammonium chloride solution for chemical activation, followed by pyrolysis at 350°C for 30 minutes. The adsorption capacity of ARHC was highest at pH 3 for both metals, at a dosage of 0.5 g, metal concentrations up to 80 mg/L and adsorption duration of 90 minutes. The research concluded that activated rice husk carbon is a more effective adsorbent than inactivated RHC for eliminating Pb and Cd

from water solutions, with a higher removal efficiency under acidic conditions for ARHC. The authors recommended that further studies could explore optimizing the activation process and investigating other heavy metals.

Adamu and Adie (2020) evaluated the effectiveness of activated carbon derived from rice husk in adsorbing Pb^{2+} ions from water solutions. They aimed to optimize parameters such as adsorbent dosage, lead concentration, contact time, temperature and pH to understand their impact on the adsorption process. The study also analyzed the adsorption kinetics, isotherms and thermodynamics of the adsorption process. The carbonized material was then impregnated using 1 mole per liter solution of H_3PO_4 at a 2:1 ratio, stirred constantly for 3 hours and subsequently oven-dried for 4 hours. The study demonstrated that ARHC is extremely efficient in adsorbing Pb^{2+} ions from aqueous solutions. Optimal removal efficiency (99.8%) was achieved under acidic conditions (pH 4) at a contact time of 10 minutes and 1.0 g of adsorbent. The authors recommended further studies to explore examining different activation methods to increase the adsorption capability of ARHC.

Haruna et al. (2020) aimed to evaluate the efficiency of three different activating agents - H_2SO_4, $ZnCl_2$ & H_3PO_4 during the process of generating activated carbon from rice husk. They investigated the influence of these agents on various properties of the resulting activated carbon such as moisture content, surface area, volatile matter content, ash content, pH and fixed carbon content. After carbonization, the samples were activated using H_2SO_4, $ZnCl_2$ or H_3PO_4 in a 1:2 ratio, followed by drying at 110°C and 200°C. Phosphoric acid was found to be the most efficient activating agent for generating highly porous activated carbon from rice husk, as it led to the greatest

surface area and the lowest ash content. $ZnCl_2$ and H_2SO_4 also produced activated carbons with acceptable surface areas, but H_3PO_4 provided superior results for adsorption applications. The authors recommended that further research could explore optimizing other factors, such as activation period and thermal conditions, to improve the properties of activated carbon.

Chiu and Lin (2019) explored a novel single-step activation process to synthesize activated carbon using waste coffee grounds for use in symmetric supercapacitors. Six different activating agents i.e., phosphoric acid, potassium hydroxide, zinc chloride, sodium hydroxide, hydrochloric acid, and iron (III) chloride were tested to understand their impact on the surface area, porosity and electrochemical performance of the activated carbon. The coffee grounds were treated with each activating agent at high temperatures (700°C for 2 hours) in a nitrogen atmosphere. The study concluded that potassium hydroxide is the most efficient agent for activating carbon from waste coffee grounds. The one-step activation process successfully enhanced the carbon's surface area and porosity, leading to a high electrochemical performance in supercapacitors. The authors recommended further investigation into optimizing the concentration of potassium hydroxide and exploring its application in other energy storage devices.

Kane et al. (2016) investigated how H_3PO_4 and KOH affect the performance of RHC for adsorbing sodium lauryl sulfate and chrome metal. The goal was to produce activated carbon exhibiting high adsorption capacity for these pollutants. The RHC was treated with H_3PO_4 and KOH at different concentrations (H_3PO_4: 30-70%; KOH: 40-80%). ARHC was tested for sodium lauryl sulfate adsorption using ultraviolet-visible (UV-Vis) spectrophotometry. Chrome metal adsorption was tested using atomic

absorption spectroscopy after surfactant-modified activated carbon was put into chrome-containing solutions. H_3PO_4 was slightly more effective than KOH in the production of activated carbon for the adsorption of sodium lauryl sulfate and chrome metal. The adsorptive capacity of carbons activated with H_3PO_4 and KOH showed little to no change with increasing concentrations of activating agents.

Youssef et al. (2015) explored the synthesis of rice husk-derived activated carbon for Pb^{2+} ion adsorption from aqueous solutions. The study focused on understanding the influence of activation methods, temperature, pH and contact time on the adsorption process. Activated carbon was produced utilizing both physical (by steam activation) and chemical techniques (using sodium hydroxide), with some samples oxidized with concentrated nitric acid to modify their surface properties. Adsorption studies were performed to examine the impact of contact time, temperature and pH on lead adsorption. The study demonstrated that rice husk-derived activated carbon, particularly when produced via chemical activation and oxidized, serves as an effective adsorbent for eliminating lead from water-based solutions. The adsorption was favored at pH 5.0 and 2 hours for Lead adsorption to reached equilibrium. The authors suggested further exploration of other activation agents and optimization of operational experimental conditions including adsorbent dosage, contact time and particle size to enhance the performance of ARHC for elimination of heavy metals from water.

Raikar et al. (2015) carried out an experimental investigation on the application of rice husk in its natural and activated forms to eliminate Pb^{2+} ions from water solutions. They tested four different adsorbents: natural rice husk (RH), rice husk ash (RHA), rice husk modified using phosphoric acid (PRH) & rice husk treated with acetic acid (ARH). The

study evaluated the impact of various parameters, such as contact time, pH, adsorbent dosage and adsorbate concentration on the adsorption process. To produce activated adsorbents, samples were soaked in phosphoric acid (0.1N) for 36 hours and carbonized at 650°C for 90 minutes, treated similarly with acetic acid (0.5N). Batch adsorption analyses were conducted by modifying parameters like contact time (60-180 minutes), pH (3-7), initial lead concentration (10-50 mg/L), and adsorbent dosage (1g - 4g). Highest Pb^{2+} ions elimination efficiencies were 93.36% (RH), 94.8% (RHA), 96.72% (PRH), and 99.35% (ARH). Pb^{2+} ions removal was higher at lower initial lead concentrations, with the efficiency decreasing as concentration increased. Pb^{2+} ions removal increased with longer contact time, reaching equilibrium at around 150-180 minutes. Increased adsorbent dosage improved Pb^{2+} ions removal efficiency. ARH achieved the highest removal (99.35%) at a dosage of 4g. Among the adsorbents, acetic acid-treated rice husk (ARH) showed the highest lead removal efficiency. The authors recommended exploring different chemical treatments to optimize adsorption performance.

Sahira et al. (2013) explored the effects of various activating agents i.e., potassium hydroxide, sulfuric acid, Iron (III) chloride, magnesium chloride and calcium chloride on the properties of activated carbon derived from Lapsi seed stone. They aimed to determine which activating agent produced activated carbon with the highest adsorption capacity iodine and methylene blue. The process of activation involved heating the mixture in the presence of the activating agent, washing using purified water, and drying the sample to obtain the final activated carbon. The present study concluded that the selection of activating agent significantly affects the adsorption capacity and surface characteristics of the activated carbon. KOH was discovered to produce activated

carbon with the highest ability to adsorb both iodine and methylene blue. Authors recommended further research into optimizing other variables influencing the effectiveness of activated carbon, like particle size, dosage of adsorbent, pH & activation temperature, to enhance adsorption capacity for various applications.

Zakir (2013) investigated the removal of Pb^{2+} ions and Cu^{2+} ions from aqueous solutions employing rice husk-derived activated carbon. The unique aspect of the study was the use of ultrasonic irradiation (sonication) to evaluate its effects on the process of adsorption. The study compared the adsorption efficiencies under normal (silent) conditions and with ultrasonic assistance. The rice husk was carbonized at 300°C and 400°C for 2 hours. The rice husk, after being carbonized, was subsequently impregnated with a 10% $ZnCl_2$ solution for 24 hours. The Pb^{2+} and Cu^{2+} ion removal was evaluated at varying concentrations between 2 and 50 mg/L in aqueous solutions. Adsorption was conducted both with and without sonication. For sonication, an ultrasonic cleaner operating at 40 kHz was used. Sonication significantly improved the adsorption performance of the activated carbon for both Pb^{2+} ions and Cu^{2+} ions. The Langmuir model more accurately illustrates the experimental data compared to the Freundlich model, indicating monolayer adsorption on a homogeneous surface. The authors recommended further studies on the effects of sonication in real wastewater systems, as well as investigations into other potential adsorbents and operating conditions. They also suggested exploring the combination of sonication with other adsorption-enhancing techniques to optimize elimination of toxic metals from contaminated water.

Taha et al. (2011) examined the adsorption potential of rice husk-based activated carbon for removing three trace metal ions (Ni^{2+}, Zn^{2+}, and Pb^{2+}) from aqueous solutions. They examined how the carbonization temperature of the rice husk impacted the resulting activated carbon's adsorption capacity for these metals. The rice husk underwent chemical treatment with 1.0 M NaOH and allowed to sit overnight at room temperature. After washing and drying, the rice husk was carbonized under three temperature conditions of 400°C, 600°C, and 800°C. Separate solutions of Ni^{2+}, Zn^{2+}, and Pb^{2+} (each at 25 ppm) were prepared, and 0.1 g of the activated carbon was introduced to 25 mL of each solution. The mixtures were agitated at room temperature, and the adsorption of each metal ion was determined over time. The activated carbon's adsorption capacity showed an increase with carbonization temperature. Rice husk subjected to carbonization at 800°C yielded the greatest adsorption capacity, followed by rice husk carbonized at 600^{o}C and 400^{o}C. Among the three metals, Pb^{2+} ions had the highest removal percentage across all samples, with 98.8% removal using ARHC carbonised at 800^{o}C. The authors recommended further investigation into the selective adsorption behavior of activated carbon derived from rice husk, particularly when multiple metal ions are present in solution simultaneously.

2.7.2 Gaps in previous studies

Past studies did not emphasize the influence of the concentration of activating agents on removal of lead ions from water using ARHC, they did not explore the potential of optimization of activating agents for the specific extraction of Pb^{2+} ions from water. Furthermore, past studies have not used the optimal impregnation/mixing ratio, activating temperature and activating time during the preparation of ARHC for extraction of Pb^{2+} ions from water.

Kane et al. (2016) tried to optimize activating agents, but their study focused on the adsorption of sodium lauryl sulfate and chrome metal rather than removal of Pb^{2+} ions from water. Furthermore, the study used very high concentrations of activating agent (H_3PO_4: 30-70%; KOH: 40-80%) which are too expensive for real life situation of treating water. Also, the ARHC was not prepared at optimal conditions i.e., impregnation/mixing ratio, activating temperature and activating time.

Therefore, this research addresses a significant gap by focusing on Pb^{2+} ions removal from water using RHC activated with a wide range of concentrations of H_3PO_4, KOH and $ZnCl_2$ and also using optimum conditions during preparation of the ARHC. This combination of focus areas has not been fully explored in the past studies, ensuring that this study contributes new knowledge to the field.

2.8 Factors influencing the adsorption of heavy metals from solution

2.8.1 Concentration of activating agent

Many prior studies such as (Kane et al., 2016), (Chiu and Lin, 2019) and (Khashan and Mohammad, 2022) focused on the removal of metals through adsorption with activated agricultural waste like nutshells and rice residues, primarily at significantly high concentrations applicable to industrial waste. Due to the common nonlinearity of metal adsorption isotherms, these previous findings may not directly apply to the context of stormwater or water treatment (Van Lienden et al., 2010).

The textural properties of activated carbon, including surface area, pore volume, and micropore volume increase with increase in KOH concentration until the optimal level is reached (Harimisa et al., 2022).

2.8.2 Adsorbent dosage

When the adsorbent dosage is raised, there is an increase in the quantity of adsorption-accessible active sites, resulting in improved adsorption potential (Kaushal, 2017). It is evident that as the dosage is raised, the percentage of removal shows a consistent increase until it reaches its peak at a dosage of 1.0 g/250ml of activated carbon. The escalation in removal efficiency with higher dosages can be explained by the expanded surface area of the adsorbent. Additionally, a higher dosage of the adsorbent signifies an higher number of adsorption sites, facilitating the adsorption of a greater quantity of lead ions (Yarkandi, 2014).

Conversely, as the quantity of adsorbent used is increased, the adsorption performance declines. It is crucial to highlight that the Pb^{2+} ions concentration remains constant while the dosage of the adsorbent rises. The potential factor contributing to this decrease in adsorption capacity could be particle aggregation, causing a decrease in the overall surface area of the adsorbent (Vijayaraghavan et al., 2006).

2.8.3 Contact time

The efficiency of removing all metal cations increases with respect to time. Initially, the adsorption of metal ions shows a steep increase, but this rate of increase slows down after sometime (Shariful et al., 2018). The initial stage of adsorption proceeds at a fast rate due to the presence of open adsorption sites, facilitating easy interaction with Pb^{2+} ions. During the first hour of contact, a significant quantity of Pb^{2+} ions is removed, followed by a gradual increase until reaching equilibrium at the two-hour mark (Yarkandi, 2014).

2.8.4 Initial metal ion concentration

Increasing the concentration of metal ions results in a decrease in adsorption capacity. This is because the biomass can adsorb more metal ions at lower equilibrium concentrations compared to higher concentrations (Kaushal, 2017). As the initial Pb^{2+} ion concentration rises, the percentage of lead (II) ions removal decreases (Yarkandi, 2014). However, the amount of metal ions adsorbed per unit mass of adsorbent (q) remains high at elevated concentrations when activated carbon is employed.

2.8.5 pH

Shariful et al. (2018) carried out adsorption experiments within a pH between 1 and 6, adjusting the pH of the metal ion solution using hydrochloric acid. Beyond a pH of 6, metal ions have the potential to create either a metal hydroxide species that can dissolve or a metal hydroxide precipitate that is not soluble. Therefore, it is advisable to perform adsorption experiments in an acidic environment to prevent the deposition of metal ions.

2.9 The process of adsorption

Typically, the adsorption mechanism of ionic metals on the adsorbent's hydrophilic surface mainly involves ion exchange or electrostatic interaction (Kane et al., 2016). Adsorption process takes into account various factors that influence it, including the dosage of activated carbon, temperature, contact time and pH of the solution, and the initial concentration of metal ion (González, 2019). Adsorption equilibrium occurs when the molecule's attachment rate on a surface matches its detachment rate, achieving a balanced state. The fundamental idea behind adsorption involves the adsorption

isotherm, which represents the equilibrium correlation between the quantity of substance attached and the fluid's density in the overall volume while maintaining a consistent temperature. The most common adsorption isotherms models used for aqueous solutions are Langmuir and Freundlich models (Kaushal, 2017).

2.9.1 Adsorption isotherms and statistical analysis

Adsorption isotherms are mathematical representations utilised to demonstrate the relationship between the amount of adsorbed material and the liquid's concentration, all while maintaining a consistent temperature (Kaushal, 2017). The understanding of the process of adsorption is greatly enhanced by isotherm studies, where the outcomes are typically represented through a graph illustrating the correlation between the quantity of adsorbed chemical substance (mg/g) and the concentration that remains (mg/L) and this plot plays an essential function in understanding the adsorption phenomenon effectively (Almohammadi and Mirzaei, 2016). The Langmuir model proves to be a more suitable match for describing Pb^{2+} ions adsorption in contrast to the Freundlich model, because the linear Langmuir regression fits have higher correlation coefficients compared to the Freundlich plot. (Youssef et al., 2015). Also, Langmuir is often linked with chemisorption where ions bind chemically to specific sites - consistent with how heavy metals like Pb^{2+} interact with functional groups on adsorbents.

2.9.2 Equilibrium adsorption isotherm

The isotherm information is acquired by creating a graph that shows the amount of Pb^{2+} ions adsorbed onto the adsorbent (mg/g) in relation to the concentration of Pb^{2+} ions that are left in the solution (mg/L). These equilibrium isotherms demonstrate how the material that adsorbs and the substance being adsorbed interact. Analysing

experimental results in comparison with an adsorption model helps understand the adsorption process mechanisms. The Pb^{2+} ion adsorption can be described using Langmuir isotherm model (Youssef et al., 2015).

2.9.3 The Langmuir isotherm

The Langmuir isotherm represents a fundamental idea in surface chemistry, elucidating the process of molecules adhering to a solid surface through adsorption. It was introduced by Irving Langmuir in 1916 as a model to explain how gas molecules adhere to a solid surface. The Langmuir isotherm postulates that adsorption occurs within a single molecular layer, meaning that only one layer of molecules can be adsorbed onto the surface.

The Langmuir adsorption isotherm (Armbruster and Austin, 1938) operates under the presumption that the process of adsorption occurs exclusively at distinct uniform (homogenous) sites within the adsorbent. This assumption greatly simplifies the determination of adsorption capacities across different scenarios. The Langmuir isotherm can be articulated in linear format as follows:

$$\frac{C_e}{q_e} = \frac{1}{q_{max}K_L} + \frac{C_e}{q_{max}} \quad \text{.....(2.1)}$$

where;

q_e = amount of adsorbate adsorbed per unit mass of adsorbent at equilibrium (mg/g).

q_{max} = maximum adsorption capacity (mg/g).

K_L = Langmuir adsorption constant (L/mg), related to the affinity of the binding sites.

C_e = equilibrium concentration of the adsorbate in the solution (mg/L).

When plotting $\frac{C_e}{q_e}$ against C_e, a linear relationship with a slope of $\frac{1}{q_{max}}$, and an intercept of $\frac{1}{q_{max}K_L}$, is observed, representing a straight line.

Interpretation of the Langmuir isotherm

i) Maximum adsorption capacity (q_{max}): This denotes the total quantity of lead ions that can be captured on the activated rice husk carbon when the adsorbent surface is entirely occupied by lead ions.

ii) Langmuir adsorption constant (K_L): This constant provides an indication of how strongly the lead ions are bound to the adsorbent. A higher K_L value indicates stronger adsorption (El Jery et al., 2024).

Among the important features of the Langmuir isotherm can be described by the separation factor, R_L also known as the dimensionless equilibrium parameter (Eq. 2.2). It is a crucial criterion applied to evaluate the favorability of adsorption process. It is defined as:

$$R_L = \frac{1}{1+K_L C_0} \quad \text{.....(2.2)}$$

where;

C_0 = is the initial concentration of the adsorbate (mg/L).

R_L = separation factor (unitless).

K_L = Langmuir adsorption constant (L/mg), related to the affinity of the binding sites.

The value of R_L indicates the nature of the adsorption process:

i) If $R_L > 1$: The adsorption is unfavorable.

ii) If $R_L = 1$: The adsorption is linear.

iii) If $0 < R_L < 1$: The adsorption is favorable.

iv) If $R_L = 0$: The adsorption is irreversible.

The R_L value changes with different initial concentrations C_0. Typically, for lower initial concentrations, R_L values will be closer to 1, indicating less favorable adsorption at very low concentrations. For higher initial concentrations, R_L values decrease, indicating more favorable adsorption as more adsorbate is available for binding. Understanding R_L helps in designing adsorption systems. Favorable R_L values (between 0 and 1) suggest that the adsorbent is effective and the process can be optimized for different concentration ranges (Modeling et al., 2024).

The Coefficient of Determination (R^2) indicates the degree of agreement between the model and the experimental data. R^2 measures the goodness of fit, ranging from 0 to 1;

i) $R^2 = 1$: Perfect fit

ii) $R^2 = 0$: No correlation

iii) $R^2 < 0$: Poor fit or negative correlation

2.10 Characterisation of the physical surface structure of the ARHC

The surface morphology refers to the physical shape, texture and distribution of materials at a surface; therefore, characterisation of surface morphology of the activated RHC involves qualitative analysis of its shape, surface features and pore size distribution (Youssef et al., 2015). Scanning Electron Microscopy (SEM) offers insights into the structure and surface features of the adsorbent material. Consequently, SEM is utilised to analyse and contrast the shapes of carbonised rice husk and the resulting activated carbon samples, offering a high-resolution view for enhanced observation of surface structure and improved identification of pore characteristics (Oribayo et al., 2020). The SEM images reveal the physical shape of the specimens, illustrating that activated carbon exhibit shapes that lack uniformity or consistent patterns (Youssef et al., 2015). The operation of SEM involves the utilisation of a concentrated electron beam to examine the surface of a specimen, and the interactions between the electrons and the sample generate various signals that can be used to create highly detailed images (Dada et al., 2022). It is important to highlight that although SEM offers significant insights into the physical features of activated carbon's surface, like its shape, texture, and roughness, as well as its structural aspects like pore size distribution and arrangement, a comprehensive and quantitative understanding of its properties may necessitate the use of additional analytical methods such as Brunauer-Emmett-Teller for specific surface area and Barrett-Joyner-Halenda technique for pore volume (Liu et al., 2020).

2.11 Instrumentation

2.11.1 Inductively coupled plasma-optical emission spectroscopy (ICP-OES)

The ICP-OES stands as a formidable method for analysing metals in diverse sample matrices. In this approach, various nebulizers or sample introduction methods are employed to inject liquid samples into an argon plasma induced by radiofrequency (RF) (Chojnacka et al., 2018). It is a method of elemental analysis employing analytical techniques. It operates by utilising a high-temperature plasma source to atomise and excite samples for qualitative and quantitative elemental analysis, the process involves exciting a sample with inductively coupled plasma to ionise its atoms. When these ions re-emit energy as light, the spectrometer analyses the emitted light, providing details regarding the elemental makeup of the sample. This method is highly capable of detecting elements at extremely low concentrations across a broad range of materials (Przybyła et al., 2022)

2.11.2 Scanning electron microscope (SEM)

A SEM generates images of a specimen by directing a concentrated electron beam across its surface. A SEM is a powerful instrument used for imaging and analysing the surface of materials at very high magnifications. It operates by employing a stream of electrons to examine the surface of the sample, providing incredibly detailed images of the surface of the sample. It helps visualize pore structures, surface texture, and cracks or granularity (Ali et al., 2023).

2.11.3 pH meter

A pH meter is an electrical instrument designed for gauging alterations in hydrogen-ion activity within a solution, indicating variations in its acidity or alkalinity. A pH meter is an analytical instrument consisting of a specialized measurement probe, which can be either a glass electrode or an ion-selective field-effect transistor (ISFET) in specific instances. The probe is connected to an electronic meter, displaying the pH measurement in decimal format. Before employing the pH meter, it is necessary to calibrate it using buffer solutions with predetermined hydrogen ion activity. Its function relies on the idea that the pH of a solution is established using the concentration of hydrogen ions within it (Cheng et al., 2005).

2.11.4 Pyrolyzer

Pyrolyzer is a device used to perform pyrolysis, a process in which organic substances are heated without the availability of oxygen, resulting in the breakdown of the material into less complex compounds, typically gases, liquids, and solid residues. In the absence of oxygen, combustion is inhibited and instead facilitates the breakdown of the material through heat. Pyrolysis is the heating of an organic material, such as biomass, without the presence of oxygen. The pyrolyzer operates under controlled temperatures and conditions to thermally degrade various materials (Serio et al., 2002).

CHAPTER THREE: MATERIALS AND METHODS

The chapter has information about materials that were used in the research including rice husk and activating agents. It covers the methods used for the various specific objectives such as carbonisation of rice husk, activation of rice husk using chemical agents and experiments for adsorption of Pb^{2+} ions.

3.1 Materials and reagents

Prior to preparations, all glasses were first washed with nitric acid followed by purified water. Nitric acid is a strong oxidizing agent that effectively removes trace metal ions, organic residues, and inorganic salts that may be present on the glass surface.

3.1.1 Preparation of solution containing Pb^{2+} ions

Materials used

i) Lead (II) nitrate ($Pb(NO_3)_2$) as a source of Pb^{2+} ions
ii) Distilled water
iii) A balance for measuring the mass
iv) A volumetric flask (1 Liter capacity)
v) Magnetic stirrer
vi) Personal protective equipment (gloves and laboratory coat)

Procedure

250 ppm (mgL^{-1}) concentration of Pb^{2+} ions in solution was prepared using the following procedure;

The required mass of lead (II) nitrate ($(Pb(NO_3)_2$) was calculated as follows; the molar mass of $Pb(NO_3)_2$ was: $Pb(NO_3)_2 = 207.2(Pb) + 2 \times 14.01(N) + 6 \times 16(O) = 331.2 gmol^{-1}$. For $250 mgL^{-1}$ Pb^{2+} ions, the amount of $Pb(NO_3)_2$ needed was calculated using the molar ratio and the 1000 ppm (mgL^{-1}) concentration as shown below:

$$250\ mg/L\ X \frac{331.2g/mol}{207.2g/mol} = 399.6 mgL^{-1}\ (or\ 0.3996 gL^{-1})$$

Using a balance, 0.3996 grams of high-purity lead (II) nitrate was accurately weighed. Lead (II) nitrate was dissolved by adding 500 mL of distilled water to the 1-liter volumetric flask and the weighed lead (II) nitrate slowly added to the water. The solution was stirred with a magnetic stirrer as shown in figure 3.1 until the lead (II) nitrate was completely dissolved. After the lead (II) nitrate is fully dissolved, more distilled water was introduced into the volumetric flask up to the 1-liter mark. The solution was thoroughly mixed by inverting the volumetric flask several times.

Figure 3.1: A magnetic stirrer.

3.1.2 Preparation of KOH

1 liter of KOH solutions of various concentrations (1%, 2.5%, 5%, 7.5%, and 10%) was prepared using the following procedures:

a) Materials used

i) KOH pellets

ii) Distilled water

iii) Analytical balance

iv) 1-liter volumetric flasks

v) Magnetic stirrer

vi) Safety equipment: gloves, goggles, and lab coat

b) Calculations

Concentration is given as a percentage weight/volume (% w/v), which means grams of solute per 100 mL of solution, therefore;

i) 1% KOH solution: 1g KOH per 100 mL solution = 10g KOH per 1 liter solution

ii) 2.5% KOH solution: 2.5g KOH per 100 mL solution = 25g KOH per 1 liter solution

iii) 5% KOH solution: 5g KOH per 100 mL solution = 50g KOH per 1 liter solution

iv) 7.5% KOH solution: 7.5g KOH per 100 mL solution = 75g KOH per 1 liter solution

v) 10% KOH solution: 10g KOH per 100 mL solution = 100g KOH per 1 liter solution

c) General procedure

An analytical balance was used to accurately weigh the amounts of KOH mentioned above for each concentration. 800mL of distilled water was introduced into a clean beaker. The weighed KOH was slowly added to the water while stirring continuously using a magnetic stirrer. This process is exothermic and releases heat, so the KOH was slowly added to avoid splashing. After the KOH was completely dissolved and the solution had cooled to room temperature, the solution was introduced into a 1-liter volumetric flask. The beaker was washed with distilled water, and the wash water was transferred into the volumetric flask. To dilute to the final volume, distilled water was added to the flask up to the 1-liter mark. The flask was repeatedly inverted to ensure the solution was well mixed.

3.1.3 Preparation of $ZnCl_2$

1 liter of $ZnCl_2$ solutions of various concentrations (1%, 2.5%, 5%, 7.5%, and 10%) was prepared using the following procedures:

a) Materials used

i) $ZnCl_2$ pellets

ii) Distilled water

iii) Analytical balance

iv) 1-liter volumetric flasks

v) Magnetic stirrer

vi) Safety equipment: gloves, goggles, and lab coat

b) Calculations

Concentration is given as a percentage weight/volume (% w/v), which means grams of solute per 100 mL of solution, therefore;

i) 1% $ZnCl_2$ solution: 1g $ZnCl_2$ per 100 mL solution = 10g $ZnCl_2$ per 1 liter solution

ii) 2.5% $ZnCl_2$ solution: 2.5g $ZnCl_2$ per 100 mL solution = 25g $ZnCl_2$ per 1 liter solution

iii) 5% $ZnCl_2$ solution: 5g $ZnCl_2$ per 100 mL solution = 50g $ZnCl_2$ per 1 liter solution

iv) 7.5% $ZnCl_2$ solution: 7.5g $ZnCl_2$ per 100 mL solution = 75g $ZnCl_2$ per 1 liter solution

v) 10% $ZnCl_2$ solution: 10g $ZnCl_2$ per 100 mL solution = 100g $ZnCl_2$ per 1 liter solution

c) General procedure

An analytical balance was used to accurately weigh the amounts of $ZnCl_2$ mentioned above for each concentration. 800mL of distilled water was added to a clean beaker. The weighed $ZnCl_2$ was slowly added to the water while stirring continuously using a magnetic stirrer. $ZnCl_2$ is highly soluble in water and therefore dissolve readily. After the $ZnCl_2$ had fully dissolved, the solution was poured into a 1-liter volumetric flask. The beaker was rinsed with distilled water, and the rinse water was transferred to the volumetric flask as well. To dilute to the final volume, distilled water was added to the

flask up to the 1-liter mark. The flask was repeatedly inverted to ensure the solution was well mixed.

3.1.4 Preparation of H_3PO_4

1 liter of H_3PO_4 solutions of various concentrations (1%, 2.5%, 5%, 7.5%, and 10%) was prepared using the following procedures:

a) Materials used

i) Concentrated H_3PO_4 solution 85% weight/weight, which meant that 85% of the solution's total weight was pure H_3PO_4, and the remaining 15% was water or other components.

ii) Distilled water

iii) Analytical balance

iv) 1-liter volumetric flasks

v) Pipettes for measuring liquids

vi) Magnetic stirrer

vii) Safety equipment: gloves, goggles, and lab coat

b) Calculations

Concentration is given as a percentage weight/volume (% w/v), which means grams of solute per 100 mL of solution. Since H_3PO_4 is typically provided in liquid form, the percentage concentration was converted to volume.

c) Density and dilution calculations

The density of concentrated H_3PO_4 (85%) is approximately 1.685 gmL^{-1}. Using the formula for dilution:

$$C_1V_1 = C_2V_2 \text{ ……...…….. (3.1)}$$

where;

C_1 = concentration of the stock solution (85% or 850gL^{-1}).

V_1 = volume of the stock solution needed (mL).

C_2 = desired concentration (gL^{-1}).

V_2 = final volume (1 liter or 1000 mL).

d) Detailed preparation for each concentration

i) For 1% H_3PO_4 solution (1 Liter), the volume of 85% H_3PO_4 needed was calculated as $V_1 = \frac{1\% \, X \, 1000 \, mL}{85\%} = \frac{10}{85} = 11.8 \, mL$, 11.8 mL of concentrated H_3PO_4 was measured using a pipette.

ii) For 2.5% H_3PO_4 solution (1 Liter), the volume of 85% H_3PO_4 needed was calculated as $V_1 = \frac{2.5\% \, X \, 1000 \, mL}{85\%} = \frac{25}{85} = 29.4 \, mL$, 29.4 mL of concentrated H_3PO_4 was measured using a pipette.

iii) For 5% H_3PO_4 solution (1 Liter), the volume of 85% H_3PO_4 needed was calculated as $V_1 = \frac{5\% \, X \, 1000 \, mL}{85\%} = \frac{50}{85} = 58.8 \, mL$, 58.8 mL of concentrated H_3PO_4 was measured using a pipette.

iv) For 7.5% H_3PO_4 solution (1 Liter), the volume of 85% H_3PO_4 needed was calculated as $V_1 = \frac{7.5\%\ X\ 1000\ mL}{85\%} = \frac{75}{85} = 88.2\ mL$, 88.2 mL of concentrated H_3PO_4 was measured using a pipette.

v) For 10% H_3PO_4 solution (1 Liter), the volume of 85% H_3PO_4 needed was calculated as $V_1 = \frac{10\%\ X\ 1000\ mL}{85\%} = \frac{100}{85} = 117.7\ mL$, 117.7 mL of concentrated H_3PO_4 was measured using a pipette.

e) General procedure

The dilution formula was used to calculate V_1 for each the concentrations of H_3PO_4 (i.e. 1%, 2.5%, 5%, 7.5%, and 10%). Using a pipette, the volumes of the concentrated H_3PO_4 above were carefully measured. 800 mL of distilled was then added to a clean beaker. The measured concentrated H_3PO_4 was slowly added to the water while stirring continuously using a magnetic stirrer. This process is exothermic and releases heat, so the acid was added slowly to avoid splashing. After the concentrated acid was completely mixed with the initial water volume, the solution was poured into a 1-liter volumetric flask. The beaker was cleaned with distilled water and the rinse water was introduced into the volumetric flask. Purified water was introduced to the flask up to the 1-liter mark. The flask was repeatedly inverted to ensure the solution was well mixed.

3.1.5 Preparation of rice husk carbon

The rice husk used was sourced from Kakunyumunyu rice milling machine located in Kibuku district, eastern Uganda. After collection, the rice husk underwent a thorough washing using distilled water to eliminate any dirt, attached particles, or other impurities that might have been present. Subsequently, it was dried naturally under ambient atmospheric conditions for a period of 3 days, which helped to reduce a portion of its moisture content. Following this initial drying phase, the rice husk was completely dried in an oven (Oven-Thermostat DHG 9023A) at 105±3 ^{o}C for 12 hours to a constant weight as shown in figure 3.2 (a). Once fully dried, samples were placed in an electrical blender for grinding as shown in figure 3.2 (b). Afterwards, the samples were subsequently passed through a sieve of 2mm mesh size to acquire a precursor powder composed of particles smaller than 2 mm in size. This size was selected to ensure consistent activation and promote efficient carbonization. Particles below 2 mm facilitate better chemical penetration during activation and allow for more uniform pore formation, which is crucial for optimizing the adsorption performance of the prepared activated carbon (Haruna et al., 2020). From the resulting powder, 500 g of sample was taken for carbonisation process. The dried rice husk was then carbonised in a pyrolyzer (SK 2-2-12 TPA2, China) under a nitrogen gas atmosphere at 600 ^{o}C for 3 hours, shown in figure 3.2 (c). It was then left to cool and packed in air-tight clear cellulose bags, awaiting activation process as shown in figure 3.2 (d).

Figure 3.2: (a) Drying rice husk in an oven, (b) grinding rice husk in an electrical blender, (c) pyrolyzer used for carbonizing rice husk and (d) storing carbonized rice husk in air-tight clear cellulose bags.

3.2 Preparation of activated carbon

Activated carbon was prepared using each activating agent by subjecting 30 grams of the powder to predetermined optimal conditions through heating. The optimal conditions were impregnation ratio, soaking temperature and time, heating/activating temperature and time while varying the activating agent concentration.

3.2.1 Optimising the concentration of activating agents

Fifteen samples of 30 grams each of the powder were soaked in a suitable volume of 1%, 2.5%, 5%, 7.5% and 10% concentration (Kane, Mishra and Dutta, 2016) of activating agents such that the impregnation/mixing ratio (RHC: activating agent) was the same i.e., 1:4 for potassium hydroxide, zinc chloride and phosphoric acid (Guo et al., 2002; Liou and Wu, 2009; Li et al., 2011). The mixtures were allowed to equilibrate at room temperature for 2 hours to guarantee a uniform blend of the powder and the activating agent, ensuring that every particle comes into contact with the activating agent.

3.2.2 Optimum activating temperature and time

The samples mentioned in 3.2.1 above were heated in a pyrolyzer. For potassium hydroxide-RHC mixture, the temperature was increased to 400 °C at the rate of 10 °C/min and held for 30 min and was continued to be heated to 800 °C at 10 °C/min and maintained for 1 hour (Guo et al., 2002). For RHC treated with zinc chloride and phosphoric acid, the mixtures were heated up to 500 ^{o}C for 1 hour (Liou and Wu, 2009; Li et al., 2011). KOH-RHC mixture was heated at higher temperatures (i.e., 800 ^{o}C) because it requires more energy to chemically react with carbon, generate pores via

intercalation, and maximize surface area unlike RHC treated with H_3PO_4 or $ZnCl_2$, which activate carbon mainly through physical and dehydration processes at lower temperatures (i.e., 500 ^oC) (Diao et al., 2002; Nandi et al., 2023).

3.2.3 Final rice husk activated carbon

After cooling, samples were rinsed using distilled water adjusted to pH 7to wash out the activating agents followed by oven drying at 105±3 ^oC for 12 hours. The samples were ground by means of an electrical blender, then passed through a sieve of 149 microns mesh size as shown in figure 3.3 (a) and kept in air-tight clear cellulose bags for subsequent experimental use.

Figure 3.3: (a) Sieving of ground samples

3.3 Preparing inactivated carbon

Inactivated rice husk carbon was included in the study as a baseline or control to assess the enhancement in adsorption performance resulting from activation. By comparing the Pb^{2+} ions removal efficiency of inactivated and activated carbon, the research was able to quantify the specific contribution of the activation process and evaluate the effectiveness of different activating agents. This comparison also highlights the value of chemical activation in transforming a low-cost agricultural waste into a more efficient adsorbent.

Following the preparation of activated carbon, a pyrolyzer was used to heat 30 grams of the raw powder. This step aimed to create a sample of inactivated carbon under the optimal temperature (500 ^{o}C) and time (2 hours) conditions. This sample of inactivated carbon facilitated comparison of performance with activated carbon during adsorption studies.

3.4 Laboratory tests

The characterisation tests using the SEM were carried out in the Materials Laboratory under the College of Engineering, Design, Art and Technology of Makerere University.

Adsorption batch experiments were conducted in the Chemistry Laboratory under chemistry department, faculty of science of Kyambogo University. Then measuring of filtrate Pb^{2+} ions concentration was also conducted in the Chemistry Laboratory.

3.5 Characterisation of ARHC

The physical surface properties/ structure of both the inactivated rice husk and the ARHC were analysed using the SEM (Li et al., 2011). Through SEM imaging, the surface pore size, shape and texture were visualised. Although SEM is mainly employed for surface morphology assessment, it can offer some qualitative insights into the pore structure of the material. Therefore, SEM images were used to provide qualitative analysis of size of pore distribution and overall porosity of the activated carbon.

3.6 Adsorption batch experiments

3.6.1 Materials used

i) Adsorbents i.e., KOH-activated RHC (ARHCK), H_3PO_4-activated RHC (ARHCH), $ZnCl_2$-activated RHC (ARHCZ) and the inactivated RHC.

ii) Pb^{2+} ions solution of concentration 250 mgL^{-1}.

iii) Distilled water.

iv) Analytical balance.

v) pH meter.

vi) Magnetic stirrer.

vii) Conical flasks (250 mL).

viii) Whatman's No.1 filter paper.

ix) ICP-OES for determining the concentration of Pb^{2+} ions.

3.6.2 Experimental setup

Twenty conical flasks of size 250 mL were labeled for different KOH concentrations and adsorbent dosages. For each KOH concentration (1%, 2.5%, 5%, 7.5%, and 10%), flasks with adsorbent dosages of 0.25 g, 0.5 g, 0.75 g, and 1 g (which is same as 5g/L, 10g/L, 15g/L, and 20g/L) were prepared. The mounts of the ARHC were weighed and added to each flask.

3.6.3 Adsorption process

50 mL of the Pb^{2+} ions solution (of concentration 250 mgL^{-1}) was added to each flask. The flask was positioned on a magnetic stirrer and agitated the mixture at a steady speed of 60 rpm for a predetermined contact time of 2 hours. The experiments were conducted at room temperature (approximately 25 ^{o}C). The procedure was repeated for the rest of the flasks.

3.6.4 Filtration and analysis

After the contact time, the mixture was subjected to filtration using Whatman's number one filter paper by putting the filter paper on a funnel and placing it on a round bottom or trough, to isolate the adsorbent from the solution. From the filtrate, only 15 ml was picked in a 15 ml-size falcon tube and analyze using the ICP-OES shown in figure 3.4 (a).

3.6.5 Duplicate experiments

Each experiment was performed twice to verify accuracy and reproducibility of the results. The results were recorded and averaged from the duplicate experiments. Each experiment was conducted in duplicate to ensure basic reproducibility and reliability of

the results while optimizing the available time, resources, and materials. Although triplicate runs are often ideal for increasing statistical reliability, conducting the experiments twice allowed for the detection of significant variations or anomalies without excessively straining limited laboratory resources. This approach is commonly accepted in preliminary or comparative studies, especially when the focus is on evaluating trends, such as the relative effect of different activating agents on Pb^{2+} ion removal.

The procedure from section 3.6.2 to section 3.6.5 was repeated for ARHC activated with H_3PO_4, ARHC activated with $ZnCl_2$ and the inactivated RHC.

3.6.6 Calculation of adsorption capacity

The calculation of the quantity and percentage of adsorbed Pb^{2+} ions at equilibrium were determined using equations 3.2 and 3.3, respectively.

$$q_e = \frac{(C_o - C_e)}{m} V, \ldots\ldots\ldots\ldots\ldots\ldots\ldots\ldots\ldots\ldots\ldots\ldots\ldots\ldots \quad (3.2)$$

$$\text{Removal (\%)} = \frac{(Co - Ce)}{Co} \; X \; 100 \; ,\ldots\ldots\ldots\ldots\ldots\ldots\ldots\ldots\ldots\ldots\ldots\ldots \quad (3.3)$$

where;

q_e = amount of Pb^{2+} ion removed at equilibrium in mgg^{-1}.

C_0 = initial concentration of Pb^{2+} ions in mgL^{-1}.

Ce = equilibrium concentration of Pb^{2+} ions in mgL^{-1}.

m = mass of adsorbent used in g.

V = volume of solution used in liters.

3.6.7 Plotting and analysis of data

Microsoft excel (office 16 version) was used for data entry, processing, and statistical analysis, including calculations of adsorption capacity, removal efficiency, and graphical presentations. A graph of adsorption capacity (q_e) versus concentration of activating agent was plotted. Also, a graph of adsorption capacity (q_e) versus adsorbent dosage was plotted. The optimal concentrations of the activating agents and the dosage of adsorbent for maximum Pb^{2+} ion removal was determined by selecting the sample from each of the KOH, $ZnCl_2$, and H_3PO_4-activated RHC that gave the highest removal efficiency.

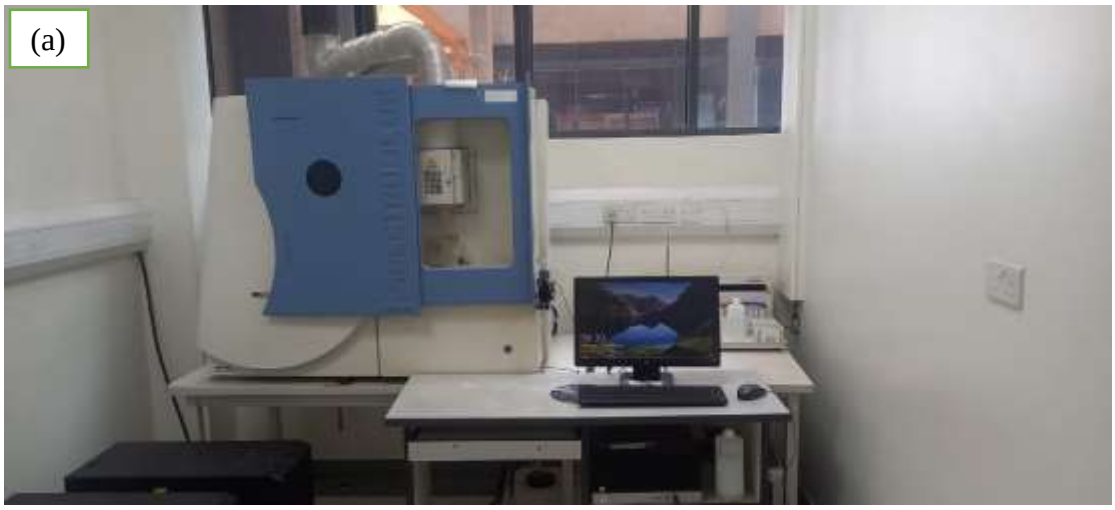

Figure 3.4: (a) The inductively coupled plasma-optical emission spectroscopy

3.6.8 Adsorption isotherm studies

To comprehend the adsorption mechanism, it was essential to utilise adsorption isotherm. An adsorption isotherm was employed to illustrate how the amount of Pb^{2+} ions adsorbed in adsorbent phase correlated with the concentration of Pb^{2+} ions in liquid phase when the adsorption process achieved a state of balance. The effectiveness of

isotherm model was examined by introducing the same known volume of Pb^{2+} ions solution with varying concentrations into a 150 mL conical flask having same known mass of adsorbent (Lakshmikandhan and Ramadevi, 2019). The conditions for this experiment included a contact duration of 2 hour, and room temperature (i.e., 25 °C). Adsorption isotherm had a vital part to play in establishing the highest adsorption capacity. The capacity of adsorption of the ARHC was assessed through the application of Langmuir isotherm. The adsorption results were applied to the Langmuir isotherm equation (equation 2.1), and OriginPro software was used to plot and fit the adsorption isotherms. Subsequently, the model constants were determined for analysis.

CHAPTER FOUR: RESULTS AND DISCUSSION

The investigation aimed to optimise the concentration of the activating agents, to characterise the surface structure of the rice husk carbon when it is both activated and not activated as well as to examine lead ion adsorption using ARHC.

The objective to characterize the surface structure of rice husk carbon, both in its activated and non-activated forms, was included to establish a scientific basis for comparing the effect of different activating agents. By analyzing both forms, the study clearly demonstrated how activation modifies the carbon structure and contributes to the increased removal efficiency of Pb^{2+} ions from water.

4.1 Optimum concentration of the activating agents

4.1.1 Percentage removal efficiency of Pb^{2+} ions by RHC activated with KOH

It can be seen from Table 4.1, Figure 4.1 and appendix Table A.1 that the removal efficiency of Pb^{2+} ions by RHC activated with KOH (ARHCK) showed a stronger and uniform interaction of Pb^{2+} ions for all the selected concentrations and dosages. Adsorption at moderate concentrations of KOH (i.e., 2.5% - 7.5%) achieved greater removal efficiency of Pb^{2+} ions by the ARHCK compared to adsorption at low (1.0%) and high (10.0%) concentrations. The maximum removal efficiency of Pb^{2+} ions was achieved at 7.5% concentration of activating agent and 5g/L dosage of the adsorbent. The RHC activated with both low and high concentrations of KOH resulted in low removal efficiency of Pb^{2+} ions. Therefore, the optimal concentration of KOH as an activating agent for preparing ARHC was taken as 7.5%, when 5g/L was used as the dosage of the adsorbent.

Table 4.1: Mean percentage removal efficiency of Pb^{2+} ions by ARHCK

Dosage (g/L)	Percentage concentration of KOH (w/v)				
	1.0%	2.5%	5.0%	7.5%	10.0%
	Mean percentage removal (%)				
5.0	91.1	99.5	98.5	99.9	99.7
10.0	84.1	88.8	95.5	94.9	90.2
15.0	63.1	93.5	94.9	94.7	90.4
20.0	43.4	94.6	88.8	94.3	64.5

The ARHCK activated at moderate concentration of 7.5% resulted in higher removal efficiency of Pb^{2+} ions from water compared to activation carried out with 1.0% and 10.0% KOH concentrations due to several reasons as explained next;

a) Optimal porosity development

At low KOH concentrations such as 1.0%, the activation process is insufficient, leading to limited chemical reaction and poor development of porosity, consequently reducing the availability of adsorption sites for Pb^{2+} ions (Song et al., 2018). At very high concentrations of KOH such as 10.0%, excessive chemical reactions can lead to the collapse or merging of pores, thereby reducing the effective surface area. This phenomenon, commonly referred to as "over-activation", results in a decrease in the availability of adsorption sites, which are critical for Pb^{2+} ions adsorption.

Moderate concentrations of KOH (i.e., 2.5% - 7.5%) strike a balance, creating an optimal pore-rich structure with an extensive surface area without causing pore collapse. This balance results in a material with a large number of micropores and mesopores, providing ample adsorption sites for lead ions (Futalan et al., 2023).

b) Ideal pore size distribution

Low KOH concentration (1.0%) leads to low activation which does not sufficiently develop the pore structure, resulting in a lower capacity for trapping lead ions. High KOH concentration leads to excessive activation causing the formation of larger pores at the expense of micropores, which are more effective for lead ion adsorption due to their size compatibility with the ions. Moderate KOH concentrations (i.e. 7.5%) promotes the formation of a well-balanced pore size distribution, with an optimal mix of micropores and mesopores that enhance the material's adsorption capacity for lead ions (Nnaji et al., 2017).

In summary, moderate KOH concentrations provide the right conditions for developing a high surface area and an optimal pore size distribution, all of which contribute to enhanced adsorption of Pb^{2+} ions from water. This concentration avoids the pitfalls of under-activation at low concentrations and over-activation at high concentrations, leading to superior adsorption performance.

4.1.2 Percentage removal efficiency of Pb^{2+} ions by RHC activated with $ZnCl_2$

As shown in Table 4.2, Figure 4.1 and appendix Table A.2, when tests were conducted using the RHC activated with $ZnCl_2$ (ARHCZ) as adsorbent, low concentrations (i.e., 1.0%) of the $ZnCl_2$ resulted in higher percentage removal efficiency of Pb^{2+} ions in comparison with tests carried out using ARHCZ of high concentration of agent. The RHC prepared using 1.0% concentration of $ZnCl_2$ and 20g/L dosage gave the maximum removal efficiency of Pb^{2+} ions and therefore, were taken as the optimal concentration and dosage respectively.

Table 4.2: Mean percentage removal efficiency of Pb^{2+} ions by ARHCZ

Dosage (g/L)	Percentage concentration of $ZnCl_2$ (w/v)				
	1.0%	2.5%	5.0%	7.5%	10.0%
	Mean percentage removal (%)				
5.0	96.0	44.5	21.1	48.8	9.0
10.0	96.5	75.6	39.8	67.0	31.8
15.0	98.2	80.8	50.4	78.0	44.5
20.0	98.5	87.6	82.5	78.2	55.5

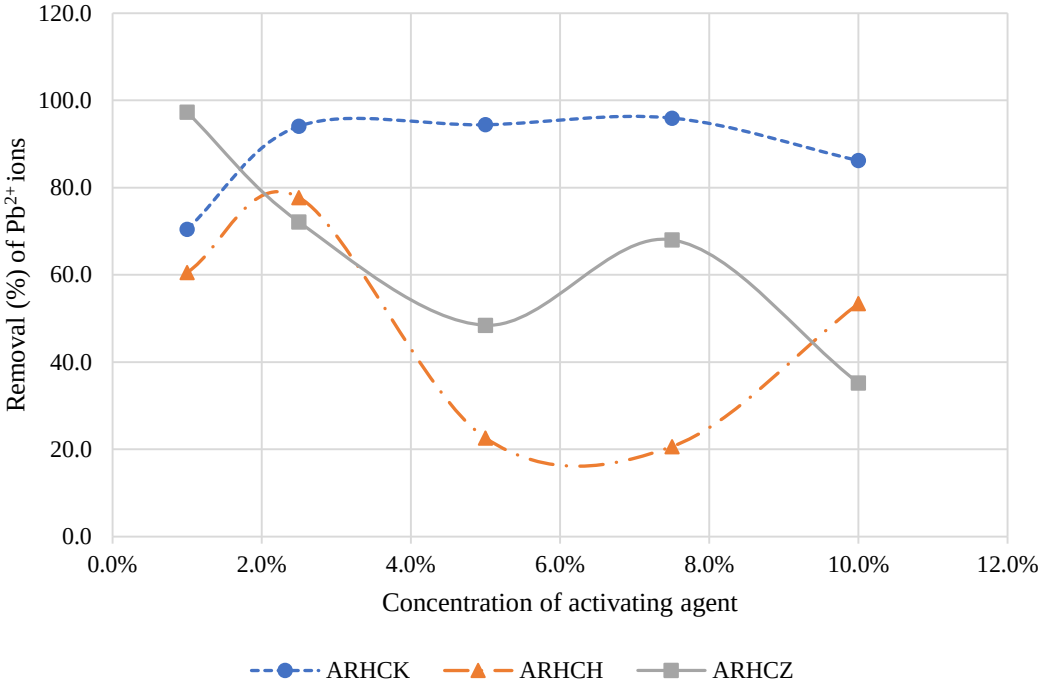

Figure 4.1: Effect of concentration of activating agent on removal (%) of Pb^{2+} ions

Similarly, the optimisation data obtained here found $ZnCl_2$ also comparably efficient but at its optimal which is in agreement with a related study on Periwinkle shell activation using $ZnCl_2$ (Gunorubon and Chukwunonso, 2018). While a considerable interaction of Pb^{2+} ions with ARHCZ existed, it only applied at the optimal level of concentration 1.0% with the peak adsorption at 20g/L. The other $ZnCl_2$ concentrations showed very poor and non-uniform adsorption abilities. Activating rice husk carbon

with a low (1.0%) concentration of $ZnCl_2$ resulted in higher removal efficiency of Pb^{2+} ions from water compared to activation with a high (10.0%) concentration of $ZnCl_2$ due to several factors related to the optimal formation of the porous structure and surface chemistry as explained next.

a) Optimal porosity development

At low concentrations (i.e., 1.0%), $ZnCl_2$ effectively promotes the formation of a well-developed porous structure with a high surface area and a balanced pore size distribution (Aroh and Aroh, 2022). This optimal porosity is crucial for providing numerous active sites for lead ion adsorption. While at higher concentrations (such as 10.0%), $ZnCl_2$ leads to over-activation, where the excessive chemical reaction can collapse the porous structure or merge smaller pores into larger ones. This reduces the surface area and the number of micropores, which are essential for effective lead ion adsorption (Alam et al., 2020).

b) Controlled pore size distribution

The 1.0% concentration of $ZnCl_2$ results in a controlled development of micropores and mesopores, which are particularly effective for trapping and adsorbing Pb^{2+} ions due to their size compatibility (Haruna et al., 2020). The presence of a higher number of appropriately sized pores increases the adsorptive capacity of the carbon. Excessive activation with high $ZnCl_2$ concentrations (such as 10.0%) often leads to the development of larger pores and a reduction in micropore volume. Larger pores are less effective in adsorbing small Pb^{2+} ions, leading to reduced overall adsorption efficiency (Ahiduzzaman and Sadrul Islam, 2016).

c) Surface functional groups

Activation with 1.0% concentration of $ZnCl_2$ introduces a sufficient number of surface functional groups (e.g., hydroxyl, carboxyl) that enhance the chemical interaction with Pb^{2+} ions (Din et al., 2017). These functional groups play a significant role in the adsorption process by binding Pb^{2+} ions via multiple mechanisms, such as ion exchange and complexation. High $ZnCl_2$ concentrations lead to the excessive formation of surface by-products and possible blocking of active sites. This reduces the availability of functional groups that are critical for effective Pb^{2+} ion adsorption, thereby decreasing the capacity of adsorption (Wang et al., 2023).

d) Chemical stability and structure integrity

At low concentration of $ZnCl_2$ (1.0%), the activation process maintains the structural integrity of the carbon, ensuring that the porosity and surface chemistry are optimized for Pb^{2+} ions adsorption without significant degradation of the material (Yahaya et al., 2010). Higher concentrations of $ZnCl_2$ (such as 10.0%) result in chemical degradation or the formation of non-porous carbonaceous residues, which negatively impact the adsorption properties of the material. Over-activation leads to a loss of structural integrity, further diminishing the adsorption efficiency (Futalan et al., 2023).

In summary, the 1.0% concentration of $ZnCl_2$ provides the right conditions for developing a highly a porous framework exhibiting elevated surface area, balanced distribution of pore sizes, and sufficient functional groups, all of which lead to enhanced adsorption of lead ions from water. Higher concentrations like 10% lead to over-activation, reducing the material's effectiveness due to pore collapse, reduced micropore volume, and potential blocking of active sites.

4.1.3 Percentage removal efficiency of Pb^{2+} ions by RHC activated with H_3PO_4

For the tests conducted using RHC activated with H_3PO_4 (ARHCH) as adsorbent (see Table 4.3 and appendix Table A.3), low concentrations of H_3PO_4 (such as at 1.0% and 2.5% concentration) achieved higher percentage removal efficiency of Pb^{2+} ions with a maximum achieved at around 20g/L dosage and 2.5% concentration of H_3PO_4. However, other concentrations for example the 5.0% and 7.5% concentrations of the H_3PO_4 achieved low removal efficiency of Pb^{2+} ions except for the 10% which was slightly above 50% removal at all dosages. Therefore, the optimal dosage of ARHCH adsorbent and concentration of the H_3PO_4 was taken as 20g/L and 2.5% respectively.

Table 4.3: Mean percentage removal efficiency of Pb^{2+} ions by ARHCH

Dosage (g/L)	**Percentage concentration of H_3PO_4 (w/v)**				
	1.0%	**2.5%**	**5.0%**	**7.5%**	**10.0%**
	Mean percentage removal (%)				
5.0	28.5	73.8	12.0	32.7	52.4
10.0	51.8	72.8	17.1	13.2	55.4
15.0	77.6	80.3	27.1	6.1	55.1
20.0	84.0	84.1	34.2	30.5	55.7

Activating rice husk carbon with lower concentrations of the H_3PO_4 e.g., the 1.0% & 2.5% resulted in higher Pb^{2+} ions removal efficiency from water compared to activation done with 5.0% and 7.5% KOH concentrations due to several reasons related to the optimal formation of the porous structure, surface chemistry, and preservation of structural integrity.

a) Optimal porosity development

The lower concentrations of H_3PO_4 such as the 1.0% and 2.5% are sufficient to create a highly porous structure with a large surface area (Okuofu et al., 2015). Phosphoric

acid serves as a dehydrating reagent & a porogen, promoting the development of a well-balanced pore structure with ample micropores and mesopores essential for effective lead ion adsorption. Higher concentrations of H_3PO_4 such as the 5% and 7.5% can lead to excessive chemical activation, resulting in the collapse or merging of pores. This over-activation reduces the overall surface area and the number of effective micropores, which are critical for trapping lead ions (Luo et al., 2019).

b) Controlled pore size distribution

The lower concentrations of H_3PO_4 such as 1% and 2.5% allow for the formation of a controlled distribution of pore sizes, with an optimal mix of micropores and mesopores (Wang et al., 2011). This structure is particularly effective for the uptake of small lead (II) ions, maximizing the adsorptive capacity. At higher concentrations of H_3PO_4, the process of activation can result in larger pores at the expense of micropores. Larger pores are less effective in adsorbing small lead ions, leading to decreased overall adsorption efficiency (Salahudeen and Alhassan, 2022).

c) Surface functional groups

Adequate activation with lower concentrations of H_3PO_4 (1% and 2.5%) introduces a sufficient number of surface functional groups, including hydroxyl and phosphate groups, which enhance the chemical interaction with Pb^{2+} ions (Huang et al., 2014). These functional groups improve the adsorption capacity through ion exchange and complexation mechanisms. Excessive activation with high concentrations of H_3PO_4 (i.e., 5% and 7.5%) can lead to the formation of too many surface by-products, potentially blocking active sites and reducing the number of functional groups available for lead ion adsorption (Yerdauletov et al., 2023).

d) Chemical stability and structural integrity

Lower concentrations of the H_3PO_4 maintain the structural integrity of the carbon, ensuring that the porosity and surface chemistry are optimized for Pb^{2+} ions adsorption without significant degradation of the material (Anon, 2017). Higher concentrations of H_3PO_4 (5% and 7.5%) can cause chemical degradation or the formation of non-porous residues, negatively impacting the adsorption properties. Over-activation can lead to a loss of structural integrity, further diminishing the adsorption efficiency (Futalan et al., 2023)

In summary, activating rice husk carbon with 1% and 2.5% concentrations of phosphoric acid provides the right conditions for developing a highly porous framework characterized by a high surface area, balanced distribution of pore sizes, and sufficient functional groups. These factors contribute to increased adsorption efficiency of Pb^{2+} ions from water. Higher concentrations like 5% and 7.5% result in over-activation, reducing the material's effectiveness due to pore collapse, reduced micropore volume, and potential blocking of active sites.

4.2 Surface structure of the rice husk carbon when it is both activated and not activated

4.2.1 Characterisation based on the SEM images

Figure 4.2 (a) of the ARHCK exhibited a highly porous and rough surface with a well-developed network of interconnected pores. This was due to the aggressive etching and chemical reactions between KOH and the carbon matrix. The surface of Figure 4.2 (b) of the ARHCH appeared more uniform compared to the surface of ARHCK. This was

because H_3PO_4 activation resulted in a less aggressive pore formation process-macropores, creating a more orderly structure. The SEM images of Figure 4.2 (c) for the ARHCZ showed a distinct pattern of mesopores. The surface was less fragmented compared to the surface of the ARHCK, indicating a different mechanism of pore development (Daffalla et al., 2012). Finally, Figure 4.2 (d) of the inactivated RHC typically showed a relatively natural texture and fewer visible pores. The structure was less porous due to the absence of chemical activation (Barakat et al., 2023).

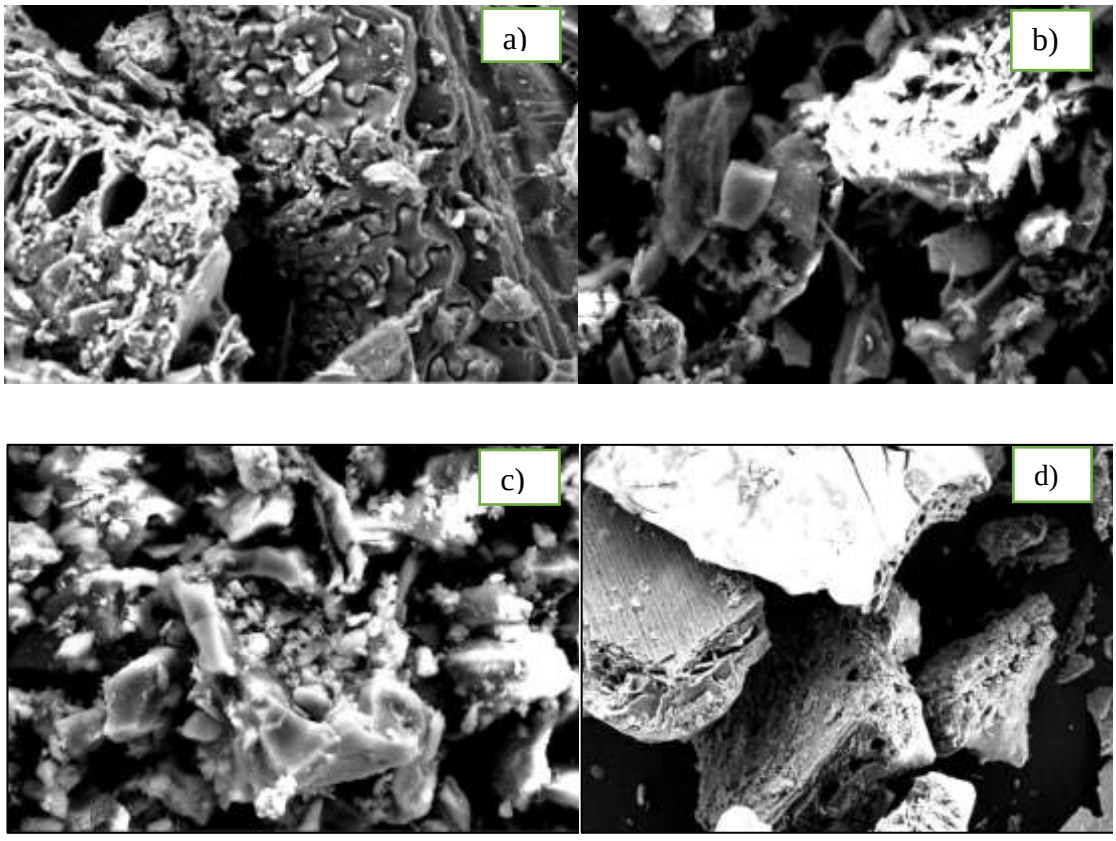

Figure 4.2: Surface texture of (a) ARHCK-interconnected pores, (b) ARHCH-macropores, (c) ARHCZ-mesopores and (d) inactivated RHC-natural texture and fewer visible pores.

The ARHCK produced a highly porous and rough surface characterized by a well-structured network of interconnected pores compared to ARHCH and ARHCZ due to the distinct mechanisms of chemical activation and the specific interactions between KOH and the RHC structure as explained next.

a) Strong dehydration and etching effect of KOH

KOH is a strong base and an effective dehydrating agent that reacts vigorously with the organic components of rice husk, such as cellulose, hemicellulose, and lignin. In the course of the activation process, KOH promotes the breakdown of these biopolymers, promoting the release of volatile substances like carbon dioxide, water vapor, carbon monoxide, methane & other light hydrocarbons (Muniandy et al., 2014). These volatiles are generated arising from thermal decomposition and chemical interactions between KOH and the carbonaceous matrix. Escape of these volatile compounds from the solid matrix results in the formation of pores & contributes to a large surface area (Bari et al., 2022). This process etches the carbon structure, creating a rough surface with a high degree of porosity. $ZnCl_2$ and H_3PO_4 also act as dehydrating agents, but their effects are less aggressive compared to KOH. $ZnCl_2$ tends to create a more uniform pore structure without the extensive etching seen with KOH. H_3PO_4, while effective in forming pores, often leads to a less interconnected pore network (Le Van et al., 2019).

b) Generation of interconnected pores

The activation process with KOH facilitates the formation of a highly interconnected network of micropores and mesopores. This network enhances the surface area and provides numerous adsorption sites, which are critical for applications like heavy metal ion adsorption. $ZnCl_2$ generally forms pores by promoting the development of a specific

type of porosity that is less interconnected. H_3PO_4 creates a more controlled and less extensive network of pores, leading to a different surface morphology (Li et al., 2015).

c) Chemical reactions and by-products

Throughout the process of activation, KOH chemically interacts with the carbon matrix to form potassium carbonate (K_2CO_3), along with other by-products such as potassium oxide (K_2O), potassium bicarbonate ($KHCO_3$), carbon dioxide (CO_2), and water (H_2O). These by-products can be removed through washing, leaving behind a highly porous carbon structure (Chen et al., 2011). The reaction also helps in creating a rough surface texture by breaking down the carbon material more extensively. Activation with $ZnCl_2$ typically leads to the formation of a more robust and less reactive carbon structure. The resulting pores are fewer in number and less interconnected. Additionally, $ZnCl_2$ can leave residual zinc compounds within the carbon matrix, affecting the overall porosity and surface roughness (Yang and Lua, 2006). H_3PO_4 tends to create a surface with well-distributed pores but does not lead to the same level of surface roughness and interconnected porosity as KOH. The acid treatment promotes cross-linking and the formation of phosphate groups, which help in stabilizing the pore structure but do not produce as highly porous and rough a surface as KOH (Alam et al., 2020).

d) Thermal and structural effects

The activation temperature and the strong chemical reactivity of KOH facilitate the breakdown of the rice husk's organic components, resulting in a highly porous and rough surface. The thermal effect, combined with the strong base action, leads to significant porosity development. Both $ZnCl_2$ and H_3PO_4 result in different thermal and chemical interactions with the carbon matrix. $ZnCl_2$ activation typically requires lower

temperatures and produces a more regular pore structure, while H_3PO_4 activation focuses more on the chemical cross-linking and stabilization of the carbon matrix, leading to different porosity characteristics (Barakat et al., 2023).

In summary, KOH activation resulted in a highly porous and rough surface with a well-developed network of interconnected pores due to its strong dehydrating and etching effects, efficient pore generation, and extensive chemical reactivity with the rice husk carbon structure. In contrast, $ZnCl_2$ and H_3PO_4 produced less aggressive pore formation and different surface morphologies, resulting in less interconnected and less rough porous structures.

4.2.2 Pore structure

a) ARHCK

As seen from Figure 4.3 (a), the ARHCK showed predominantly micropores with substantial surface area and extensive porosity. It indicated the highest surface coverage and distribution of pores with the pores evenly distributed throughout the particles' surfaces. The high pore density of the ARHCK can be explained by the oxidation reaction between carbon and the potassium hydroxide just like in a study on KOH activated carbon as explored by programmed temperature techniques (Lozano-Castelló et al., 2007).

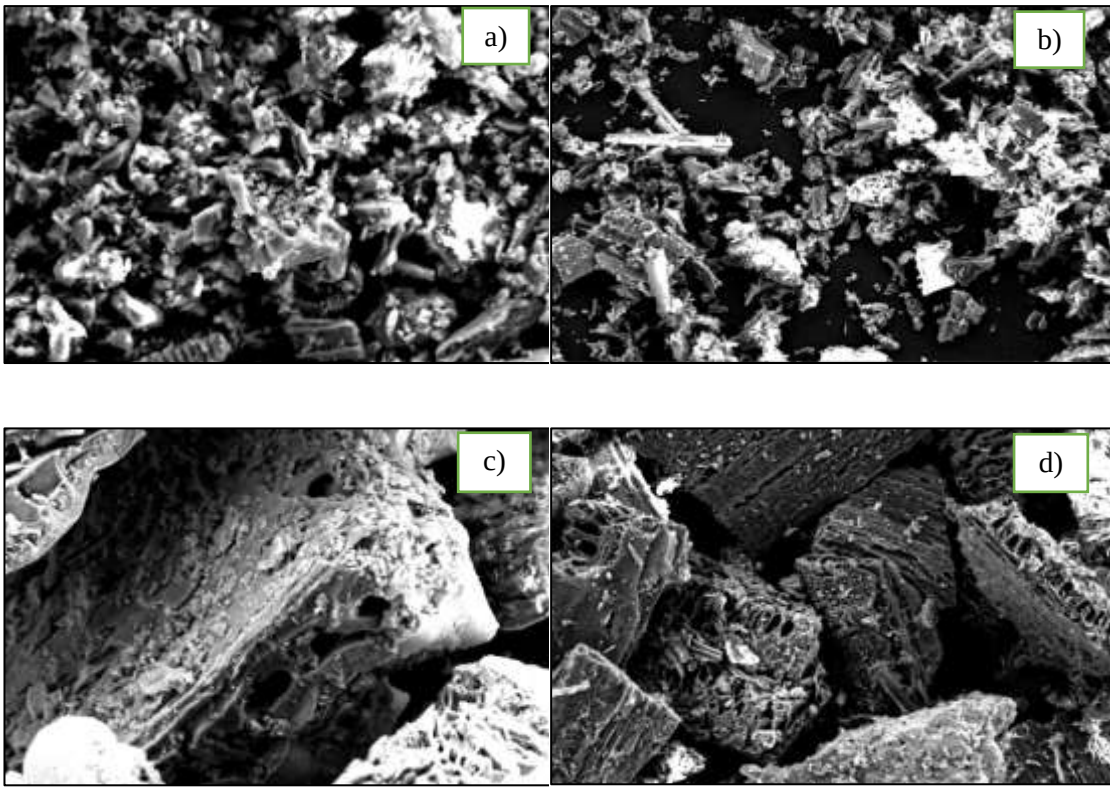

Figure 4.3: Pore count and distribution of (a) ARHCK-micropores, (b) ARHCZ-mesopores, (c) ARHCH-macropores, and (d) inactivated RHC

The reaction produces gases which lead to creation of small mesopores and numerous micropores as they escape. The suggested reaction mechanisms and pathways involving the carbon matrix and the activating agent potassium hydroxide results in production of carbon dioxide and hydrogen gases, water, metallic potassium and potassium carbonate. Therefore, the formation of a densely porous carbon matrix is as a result of these reactions and the formation of volatiles during the process of carbonization (Nandi et al., 2023). Additionally, the leaching of impurities termed as demineralization of silicate minerals from the precursor matrix improved surface pore formation (Kim et al., 2023).

b) ARHCZ

As seen from Figure 4.3 (b), the ARHCZ had a moderate pore distribution with well-developed mesopores, yielding a porous framework favourable for various adsorption applications. At the activation temperatures, zinc chloride decomposes to produce chlorine gas and zinc oxide. The chlorine gas reacts with water vapour to produce hydrogen chloride gas which reacts with the remaining cellulose and hemicellulose removing carbonaceous materials and forming pores in the process (Ozdemir et al., 2014).

c) ARHCH

A few pores were seen on the ARHCH (Figure 4.3 (c)) due to higher aggregation of the particles. Macropores were formed, but with a more uniform distribution compared to KOH activation. The pores were more defined and less extensive (Yerdauletov et al., 2023).

The proposed pore formation processes by activating the RHC with zinc chloride and phosphoric acid are the same i.e., dehydration, decomposition and etching. Both zinc chloride and phosphoric acid are dehydrating agents which remove water molecules from the cellulose and hemicellulose present in the carbon matrix that promotes the carbonisation process providing the initial framework for pore formation (Neme et al., 2022). With phosphoric acid, hydrolysis forms phosphate groups that instead cause particle agglomeration by serving as bridges as earlier discussed and this does not contribute to pore formation. The overall effect is more in the ARHCZ as compared to the ARHCH.

d) Inactivated RHC

Limited pore development, mainly macropores formed during the carbonization process. Inactivated RHC (Figure 4.3 (d)) had very few pores on the surface. As expected, there were rudimentary pore structures on the inactivated RHC surface due to the inherent porosity arising from the natural arrangement of carbon atoms in the carbon matrix (Aik Chong Lua and Guo, 2001).

e) Comparative analysis

i) Comparison between inactivated and activated RHC: Inactivated RHC had less porous surface while activated RHC (regardless of the activating agent) showed increased porosity and surface roughness.

ii) A comparative analysis was conducted among the activated rice husk carbon samples prepared using ARHCK, ARHCH and ARHCZ: The ARHCK resulted in the highest porosity and surface roughness, indicating extensive micropore formation, ARHCH produced a more uniform surface of macropores while ARHCZ generated a unique porous structure with a significant presence of mesopores.

In both cases, the surface of inactivated RHC is replaced with a rough porous uneven surface in the ARHCK, ARHCH and ARHCZ due to the activation process because of the effect of the activating agents (Gao et al., 2020). Because of the extensive etching process and numerous volatiles escaping through the carbon structure resulting from the impact of potassium hydroxide, the ARHCK surface appears more rough ,porous and irregular compared to the ARHCH and ARHCZ for whose cases the etching process

is uniform and less extensive in addition to fewer volatiles released throughout the process of activation (Xia et al., 2016).

In conclusion, the SEM images revealed significant differences in surface morphology and pore structure between the inactivated and the activated RHC, as well as among different activating agents. ARHCK resulted in the highest specific surface area and porosity, rendering it highly suitable for adsorption utilizations. ARHCH produced a more uniform surface, while ARHCZ created a unique mesoporous structure. These morphological characteristics directly influenced the adsorption properties and prospective uses of the activated carbon.

4.3 Adsorption of Pb^{2+} ions using RHC activated using various activating agents

As seen in Table 4.4 below, ARHCK demonstrated the highest percentage removal efficiency at 99.9%, making it the most efficient adsorbent owing to its high surface area and micropores, whereas, ARHCZ in contrast exhibited removal efficiency of 98.5% which is suitable for practical applications but lower than KOH. ARHCH achieved percentage removal efficiency of 84.1%, lower than ARHCK and ARHCZ due to chemical interactions provided by phosphate groups (Ternero-Hidalgo et al., 2016). The inactivated RHC demonstrated the lowest percentage removal efficiency of 53.9%.

Table 4 4: Optimal concentration of activating agents and dosage amounts of adsorbents.

Activating agent	**Optimal concentration of agent (%)**	**Optimal dosage of adsorbent (g/L)**	**Maximum percentage removal at optimal concentration and dosage (%)**
KOH	7.5	5	99.9
$ZnCl_2$	1.0	20	98.5
H_3PO_4	2.5	20	84.1
Raw RHC	N/A	20	53.9

The adsorption efficiency was highest for ARHCK, followed by ARHCZ, ARHCH and then the inactivated RHC due to several key factors regarding the properties and activation mechanisms of the activated carbons;

a) Surface area and pore structure

ARHCK resulted in the highest surface area and well-developed microporous structure. The extensive surface area offers additional active sites for Pb^{2+} ions adsorption. Additionally, the micropores created during KOH activation are particularly effective in trapping and holding Pb^{2+} ions, contributing to higher removal efficiency. ARHCZ led to a moderately high surface area with a mesoporous structure. While the surface area is lower than that of ARHCK, the mesopores were still effective in adsorbing Pb^{2+} ions, though not to the same extent as the micropores created by KOH(Alghamdi et al., 2019). Although ARHCH also has a high surface area, the pore structure includes a mix of micropores and mesopores. The specific pore structure and surface chemistry resulting from H_3PO_4 activation is less optimal for lead ion adsorption compared to KOH. In contrast, untreated RHC retains its original structure, which has fewer pores and a smaller surface area (Alghamdi et al., 2019).

b) Functional groups and chemical interactions

For ARHCK, the activation process with KOH introduces a variety of oxygen-containing functional groups such as hydroxyl, carboxyl, and carbonyl groups. These functional groups enhance the adsorption of Pb^{2+} ions through chemisorption mechanisms, providing strong binding sites. For the ARHCZ, $ZnCl_2$ activation results in the formation of acidic functional groups such as phenolic and lactonic groups. While these groups contribute to Pb^{2+} ion adsorption, they are generally less effective than the oxygen-containing groups introduced by KOH. For the ARHCH, H_3PO_4 introduces phosphate groups, which bind Pb^{2+} ions. However, the nature of these groups and their distribution is not effective in capturing lead ions as the functional groups created by KOH. Inactivated RHC has fewer surface functional groups (Loulidi et al., 2023).

In summary, the highest adsorption efficiency by the ARHCK is due to its superior surface area, highly-formulated microporous structure, as well as the presence of effective oxygen-containing functional groups that facilitate strong chemisorption. ARHCZ with its moderate surface area and mesoporous structure provides effective but lesser adsorption than the ARHCK. ARHCH also having a high surface area, has a less optimal pore structure and functional group distribution for Pb^{2+} ions adsorption compared to KOH. The lower adsorption capacity of inactivated RHC compared to chemically activated RHC is mainly owing to the latter's enhanced surface area, enhanced porosity combined with various surface functional groups. These factors collectively improve the adsorption efficiency and capacity of the activated carbons.

4.3.1 Effect of dosage of the adsorbent

Table 4.5: Average percentage removal efficiency of Pb2+ ions and dosage amounts of adsorbents.

Dosage (g/L)		**5**	**10**	**15**	**20**
%ge Removal	**ARHCK**	98	91	87	77
	ARHCH	40	42	49	57
	ARHCZ	44	62	70	80
	RAW-RHC	33	39	46	54

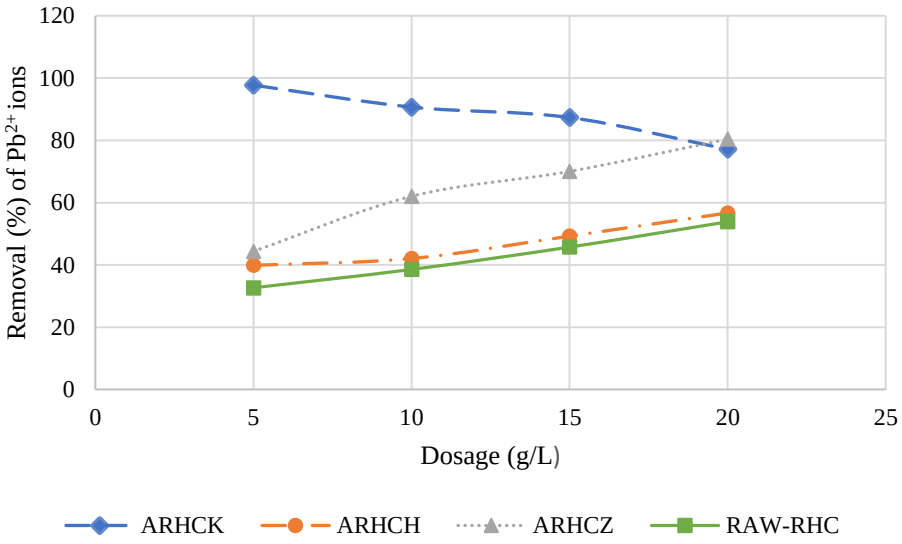

Figure 4.4: Effect of dosage of the adsorbent on the percentage removal of Pb^{2+} ions

a) ARHCK Adsorbent

Adsorption at low dosages achieved a higher adsorption capacity and vice verser with maximum achieved at around 5g/L dosage of ARHCK and 7.5% concentration of KOH. Higher dosages led to lower adsorptive capacity of the ARHCK. Therefore, the optimal dosage of the ARHCK adsorbent was taken as 5g/L at 7.5% concentration of KOH activating agent. This was because of;

i) Extensive surface area and active sites: Under low-dosage conditions, the available binding sites on the ARHCK adsorbent are more effectively utilized because the Pb^{2+} ions are more likely to encounter an available site (Yerdauletov et al., 2023). This leads to a higher percentage removal as each unit of adsorbent is more fully engaged in adsorption.

ii) Optimized adsorbent utilization: Low dosages ensure that the adsorbent surface is not saturated quickly, allowing for maximum interaction between lead ions and the adsorption sites. At higher dosages, there may be excess adsorbent, which may result in underutilization of available surface area and active sites (Futalan et al., 2023)

iii) Equilibrium conditions: Adsorption is an equilibrium process, and at lower dosages, the system is further from equilibrium, allowing for a higher driving force for adsorption. At higher dosages, the system is closer to equilibrium, and additional adsorbent fails to considerably improve the removal efficiency (Alghamdi et al., 2019).

iv) Adsorbent agglomeration: At higher dosages, there is a tendency for the adsorbent particles to agglomerate or clump together. This agglomeration reduces the effective surface area available for adsorption, thereby decreasing the overall efficiency. The individual particles are less accessible to lead ions in solution (Yerdauletov et al., 2023).

b) ARHCZ adsorbent

Tests carried out using the ARHCZ as adsorbent, low dosages of the adsorbent resulted in lower adsorption efficiency and vice verser. The adsorbent of 20g/L dosage and 1.0% concentration of $ZnCl_2$ led to the maximum adsorption capacity and therefore was take

as the optimal dosage and concentration respectively. This was due to the following reasons;

i) Surface area and active sites: At low dosages, there is a limited amount of activated carbon, leading to insufficient binding sites available for the adsorption of lead ions. $ZnCl_2$ activation typically results in a high surface area and microporous structure, which requires a sufficient quantity of adsorbent to effectively capture lead ions from the solution (Ahiduzzaman and Sadrul Islam, 2016).

ii) Adsorption saturation: When using low dosages, the available adsorbent quickly becomes saturated with Pb^{2+} ions, which reduces the overall removal efficiency. As the dosage increases, more active sites become available, preventing early saturation and allowing for a higher removal percentage (Mortada et al., 2023).

c) ARHCH Adsorbent

For the tests carried out using the ARHCH adsorbent, low dosages of the adsorbent led to lower adsorption efficiency and vice verser, with a maximum achieved at 20g/L dosage and 2.5% concentration of H_3PO_4. Therefore, the optimal dosage of ARHCH was taken as 20g/L at 2.5% concentration of the H_3PO_4. This was due to the following factors;

i) Limited active sites: At low dosages, the quantity of adsorbent is insufficient to provide a large number of binding sites required for the effective Pb^{2+} ions adsorption. H_3PO_4 activation enhances the porosity and surface area of the carbon, but these benefits can only be fully realized when there is enough

adsorbent available to interact with the Pb^{2+} ions in the solution (Alam et al., 2020).

ii) Specific surface area and pore volume: Higher dosages of ARHCH provide a larger surface area and more pores, which increases the adsorption capacity. At low dosages, the limited surface area and pore volume lead to quicker saturation of the adsorbent, reducing its overall effectiveness in removing lead ions from water (Futalan et al., 2023).

d) Inactivated RHC

Tests carried out using inactivated RHC as adsorbent, low dosages of the adsorbent led to lower adsorption efficiency and vice verser, with a maximum achieved at 20g/L dosage. Therefore, the optimal dosage of the inactivated RHC was taken as 20g/L. This was because of limited active sites since at low dosages, the quantity of adsorbent is insufficient to provide a large density of active sites required for the effective Pb^{2+} ions adsorption.

4.3.2 Langmuir adsorption isotherm

Figures 4.5 and 4.6 show Langmuir isotherms for different adsorbents i.e. ARHCK, ARHCZ, ARHCH and the Raw RHC used in the removal of Pb^{2+} ions from water. These these isotherms were essential for understanding the adsorption behavior and effectiveness of each adsorbent.

Table 4.6: Langmuir fitted isotherm parameters for adsorption of Pb^{2+} by carbon samples.

Adsorbent	**Langmuir Isotherm**			
	q_{max} (mg/g)	**K_L (L/mg)**	**R^2**	**R_L**
ARHCK	3112.86	0.261	0.993	0.015
ARHCZ	2669.52	0.218	0.990	0.018
ARHCH	2315.11	0.185	0.987	0.021
RAW RHC	1500.40	0.114	0.966	0.034

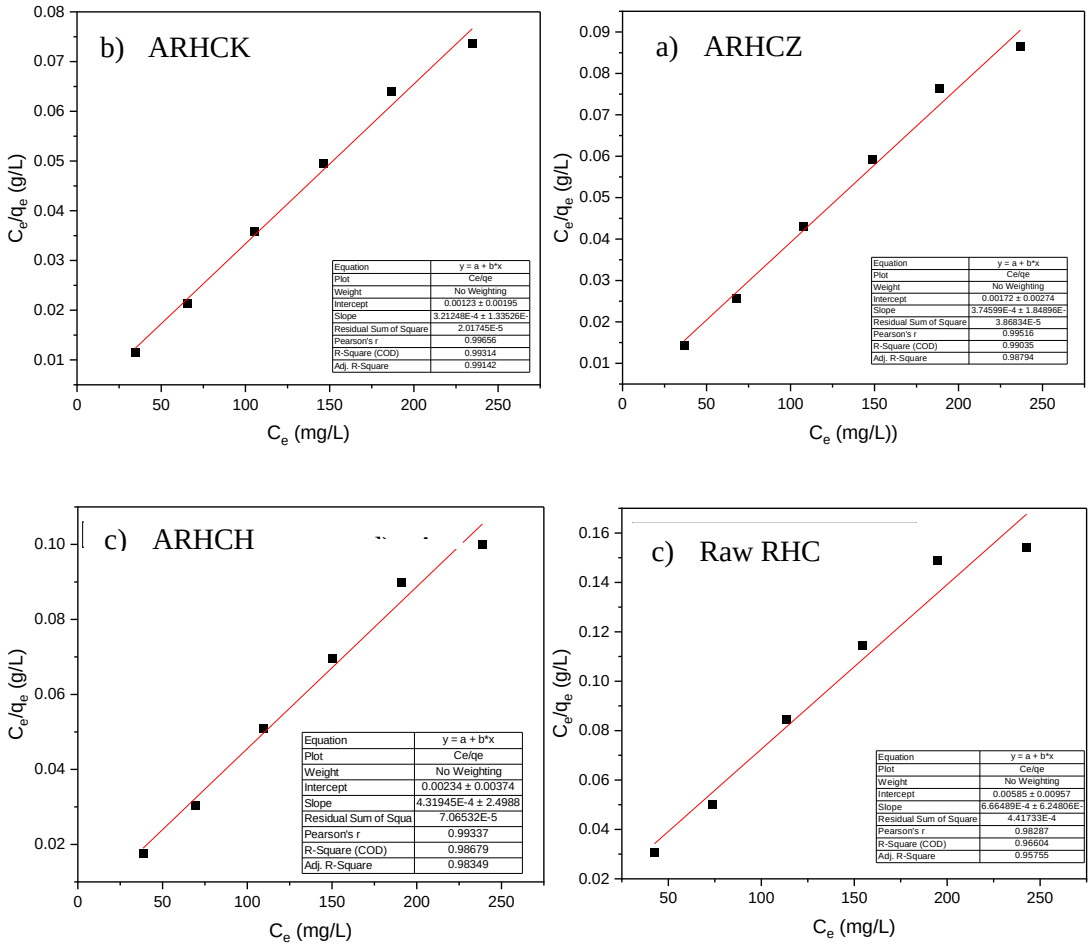

Figure 4.5: Langmuir model for (a) ARHCK, (b) ARHCZ, (c) ARHCH and (d) Raw RHC.

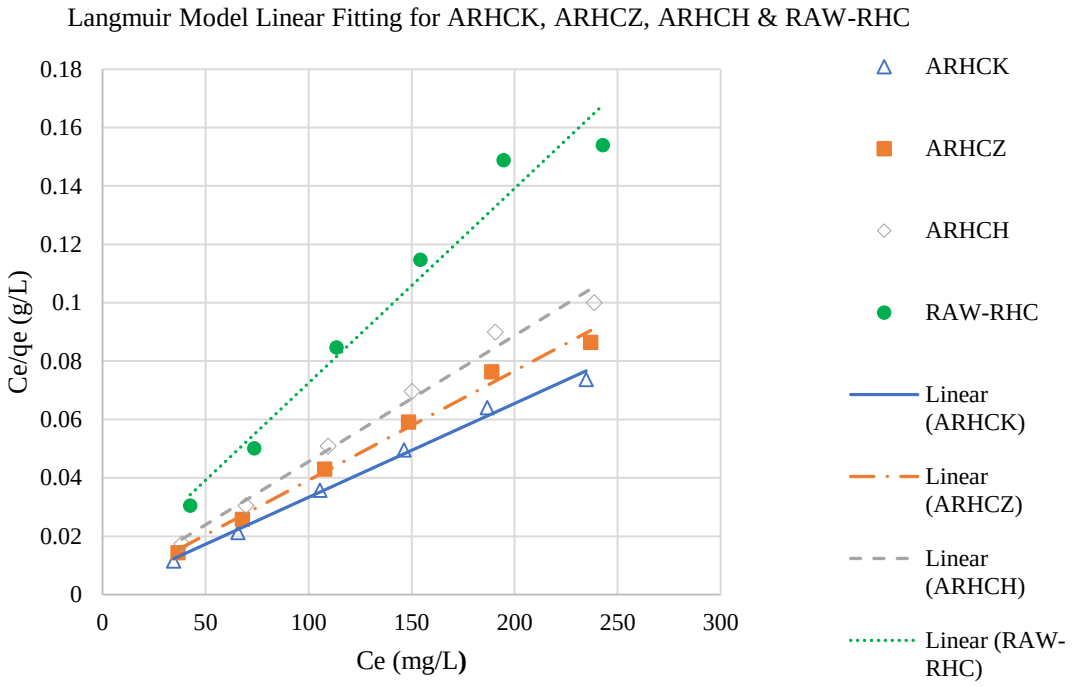

Figure 4.6: Combined Langmuir isotherm

As seen from table 4.6 above, ARHCK showed the highest adsorption capacity (q_{max} = 3112.86 mg/g) and affinity (K_L = 0.261 L/mg) for the adsorbate among the tested adsorbents. The high R^2 = 0.993 value indicated an excellent fit to the Langmuir model, confirming monolayer adsorption on a homogeneous surface. The low R_L = 0.015 value suggested highly favorable adsorption (Alam et al., 2020).

ARHCZ had a slightly lower adsorption capacity (q_{max} = 2669.52 mg/g) and affinity (K_L = 0.218 L/mg) compared to ARHCK but still performed very well. Also, the high R^2 = 0.990 value indicated a good fit to the Langmuir model while the low R_L = 0.018 indicated favorable adsorption. The ARHCH showed a moderate adsorption capacity (q_{max} = 2315.11 mg/g) and affinity (K_L = 0.185 L/mg), with a good R^2 = 0. 0.987 value indicating a reasonable fit to the Langmuir model. The R_L = 0.021 value for the

ARHCH suggested favorable adsorption conditions (Ahiduzzaman and Sadrul Islam, 2016).

Raw RHC had the lowest adsorption capacity (q_{max} = 1500.40 mg/g) and affinity (K_L = 0.114 L/mg), among the tested adsorbents. The R^2 = 0.966 value, while still high, was lower than for the activated adsorbents, indicating some deviation from the ideal Langmuir behavior. The R_L = 0.034 value was the highest among the adsorbents, indicating less favorable adsorption but still within a favorable range (Chen, 2015).

The Langmuir model provided a good fit to the data for all adsorbents, as indicated by high R^2 values. ARHCK was the most effective adsorbent with the highest q_{max} = 3112.86 mg/g and K_L 0.261 L/mg values, indicating the highest adsorption performance and affinity respectively. ARHCZ and ARHCH also showed good performance, with ARHCZ slightly outperforming the ARHCH. Raw RHC, while still effective, showed the lowest performance among the tested adsorbents (Alghamdi et al., 2019)

In summary

- The high q_{max} values for ARHCK, ARHCZ, and ARHCH indicate their potential effectiveness in practical applications for Pb^{2+} ions removal.
- The high affinity constants (K_L) for these adsorbents suggest that they can effectively remove Pb^{2+} ions even at low concentrations.
- The Langmuir model's better fit indicates that the adsorption process is likely forming a monolayer on a relatively homogeneous surface.

Among the adsorbents, ARHCK is the most effective, followed by ARHCZ and ARHCH, with Raw RHC being the least effective (Daniel Reta and Desissa, 2023). The

choice of adsorbent should consider both the adsorption capacity and affinity, as well as the specific application requirements (Uygun et al., 2023)

CHAPTER FIVE: CONCLUSIONS AND RECOMMENDATIONS

5.1 Conclusions

This present study aimed to optimise the concentration of activating agents for preparing activated rice husk carbon (ARHC), characterise the surface morphology of rice husk carbon in both activated and non-activated forms, and examine the adsorption of Pb^{2+} ions using ARHC produced with different activating agents.

Regarding the first objective, the study successfully identified the optimal concentrations of each activating agent for maximum Pb^{2+} ions removal. RHC activated with 7.5% KOH achieved the highest removal efficiency (99.9%) at 5 g/L dosage, demonstrating that KOH is highly effective in developing a microporous structure suitable for Pb^{2+} ions adsorption. RHC activated with 1.0% $ZnCl_2$ also showed a high removal efficiency (98.5%) at a higher dosage of 20 g/L, attributed to the formation of a well-balanced mesoporous structure. H_3PO_4 at 2.5% concentration attained a removal efficiency of 84.1% at 20 g/L dosage, which, although substantial, was lower than that of KOH and $ZnCl_2$ due to its less aggressive pore-forming mechanism. The inactivated RHC showed the lowest removal efficiency (53.9%), highlighting the importance of chemical activation.

For the second objective, surface characterisation using SEM images and pore distribution analysis revealed significant differences between activated and inactivated RHC. ARHCK showed the highest surface roughness and microporosity due to KOH's strong dehydrating and etching effects. ARHCZ presented a mesoporous structure with moderate roughness, while ARHCH exhibited a more uniform surface with macropores. The inactivated RHC showed a natural texture with minimal porosity.

These findings confirmed that chemical activation dramatically enhances the surface structure of rice husk carbon, improving its adsorption performance.

Concerning the third objective, the adsorption of Pb^{2+} ions was examined using ARHC prepared with KOH, $ZnCl_2$, and H_3PO_4. Langmuir isotherm modeling demonstrated that ARHCK exhibited the highest adsorption capacity (q_{max} = 3112.86 mg/g) and affinity (K_L = 0.261 L/mg), indicating monolayer adsorption on a homogeneous surface. ARHCZ and ARHCH followed with q_{max} values of 2669.52 mg/g and 2315.11 mg/g, respectively, while inactivated RHC had the lowest capacity (q_{max} = 1500.40 mg/g). The findings reaffirmed that the type and concentration of activating agent significantly influence the adsorption capacity of ARHC.

Overall, this study demonstrates that chemically activated rice husk carbon, particularly with KOH & $ZnCl_2$ at optimal concentrations, significantly enhances its structural properties and Pb^{2+} ions removal efficiency. These findings support the advancement of low-cost, effective adsorbents from agricultural waste, contributing to safe water access and aligning with Sustainable Development Goal 6 (clean water and sanitation) and Goal 3 (good health and well-being).

5.2 Recommendations

In light of the findings of this study, the following recommendations are put forward for future research and improvement of the work:

5.2.1 Investigation of regeneration and reusability.

Future studies should evaluate the regeneration potential and adsorption efficiency of the activated rice husk carbon (ARHC) after multiple cycles of use. This will help assess

the long-term viability and economic sustainability of ARHC in water treatment applications.

5.2.2 Evaluation under real environmental conditions.

Further research should be carried out under real environmental or field conditions using actual contaminated water. This would provide more practical insight into the performance of the adsorbents under conditions with competing ions and organic substance frequently present in natural water sources.

5.2.3 Comparative economic analysis of activating agents.

Although the study focused on adsorption efficiency, future work could include a comparative cost analysis of using different activating agents (e.g., KOH, $ZnCl_2$, and H_3PO_4) to determine the most cost-effective option for scaling up the application of ARHC in resource-limited settings.

5.2.4 Expansion to other heavy metals and pollutants.

Since this study focused on Pb^{2+} ions, further research should examine the effectiveness of the activated rice husk carbon in removing other toxic heavy metals including arsenic (As^{3+}), cadmium (Cd^{2+}) and mercury (Hg^{2+}), in addition to organic pollutants, to broaden its applicability.

REFERENCES

ABBAS, M.N., ALI, S.T. and ABASS, R.S. (2020) Rice Husks As a Biosorbent Agent for Pb^{2+} Ions From Contaminated Aqueous Solutions : a Review. *Biochemical and Cellular Archives*, 20(1), pp. 1813–1820.

AHIDUZZAMAN, M. and SADRUL ISLAM, A.K.M. (2016) Preparation of porous bio-char and activated carbon from rice husk by leaching ash and chemical activation. *SpringerPlus*, 5(1), 1248, DOI:10.1186/s40064-016-2932-8.

AHMAD, F., WAN DAUD, W.M.A., AHMAD, M.A. and RADZI, R. (2013) The effects of acid leaching on porosity and surface functional groups of cocoa (Theobroma cacao)-shell based activated carbon. *Chemical Engineering Research and Design*, 91(6), pp. 1028–1038.

AIK CHONG LUA and GUO, J. (2001) Preparation and characterization of activated carbons from oil-palm stones for gas-phase adsorption. *Colloids and Surfaces A: Physicochemical and Engineering Aspects*, 179(1–3), pp. 151–162.

ALAM, M.M., HOSSAIN, M.A., HOSSAIN, M.D., JOHIR, M.A.H., HOSSEN, J., RAHMAN, M.S., ZHOU, J.L., HASAN, A.T.M.K., KARMAKAR, A.K. and AHMED, M.B. (2020) The potentiality of rice husk-derived activated carbon: From synthesis to application. *Processes*, 8(2), DOI:10.3390/pr8020203.

ALGHAMDI, A.A., AL-ODAYNI, A., SAEED, W.S., AL-KAHTANI, A., ALHARTHI, F.A. and AOUAK, T. (2019) Efficient adsorption of lead (II) from aqueous phase solutions using polypyrrole-based activated carbon. *Materials*, 12(12), DOI:10.3390/ma12122020.

ALI, A., ZHANG, N. and SANTOS, R.M. (2023) Mineral Characterization Using Scanning Electron Microscopy (SEM): A Review of the Fundamentals, Advancements, and Research Directions. *Applied Sciences (Switzerland)*, 13(23), DOI:10.3390/app132312600.

ALMOHAMMADI, S. and MIRZAEI, M. (2016) Removal of copper (II) from aqueous solutions by adsorption onto granular activated carbon in the presence of competitor ions. *Advances in Environmental Technology*, 2(2), pp. 85–94.

ARBABI, M., HEMATI, S. and AMIRI, M. (2015) Removal of lead ions from industrial wastewater: Removal methods review. *International Journal of Epidemiologic Research*, 2(2), pp. 105-109.

ARMBRUSTER, M.H. and AUSTIN, J.B. (1938) The Adsorption of Gases on Plane Surfaces of Mica. *Journal of the American Chemical Society*, 60(2), pp. 467–475.

AROH, C.C. and AROH, C.U. (2022) The Influence of Activating Agents on the Properties of Activated Carbon. *International Journal of Advances in Engineering and Management*, 4(6), pp. 1093–1099, DOI: 10.35629/5252-040610931099.

AZIMI, A., AZARI, A., REZAKAZEMI, M. and ANSARPOUR, M. (2017) Removal of Heavy Metals from Industrial Wastewaters: A Review. *ChemBioEng Reviews*, 4(1), pp. 37–59.

BABATUNDE, R.I. and IBRAHIM, A.A. (2020) Removal of Heavy Metal from Waste Water Using Activated Carbon from Rice Husk. *International Journal of Advances in Scientific Research and Engineering*, 06(02), pp. 104–112, DOI: 10.31695/IJASRE.2020.33724.

BAGUMA, G., MUSASIZI, A., TWINOMUHWEZI, H., GONZAGA, A., NAKIGULI, C. K., ONEN, P., ANGIRO, C., OKWIR, A., OPIO, B., OTEMA, T., OCIRA, D., BYARUHANGA, I., NIRIGIYIMANA, E., and OMARA, T. (2022). Heavy Metal Contamination of Sediments from an Exoreic African Great Lakes' Shores (Port Bell, Lake Victoria), Uganda. *Pollutants*, *2*(4), 407–421, DOI:10.3390/pollutants2040027.

BARAKAT, N.A.M., IRFAN, O.M. and MOUSTAFA, H.M. (2023) H_3PO_4/KOH Activation agent for high performance rice husk activated carbon electrode in acidic media supercapacitors. *Molecules*, 28(1), DOI:10.3390/molecules28010296.

BARI, M.N., MUNA, F.Y., RAHNUMA, M. and HOSSAIN, M.I. (2022) Production of Activated Carbon From Rice Husk and Its Proximate Analysis. *Journal of Engineering Science*, 13(1), pp. 105–112, DOI:10.3329/jes.v13i1.60568.

BYAMBA-OCHIR, N., WANG, G.S., BALATHANIGAIMANI, M.S. and HEE MOONA. (2016) Highly porous activated carbons prepared from carbon rich Mongolian anthracite by direct NaOH activation. *Applied Surface Science*, 379, pp. 331–337.

CANALES-FLORES, R.A. and PRIETO-GARCÍA, F. (2016) Activation Methods of Carbonaceous Materials Obtained from Agricultural Waste. *Chemistry and Biodiversity*, 13(3), pp. 261–268.

CHEN, X. (2015) Modeling of experimental adsorption isotherm data. *Information (Switzerland)*, 6(1), pp. 14–22.

CHEN, Y., ZHU, Y., WANG, Z., LI, Y., WANG, L., DING, L., GAO, X., MA, Y. and

GUO, Y. (2011) Application studies of activated carbon derived from rice husks produced by chemical-thermal process - A review. *Advances in Colloid and Interface Science*, 163(1), pp. 39–52, DOI:10.1016/j.cis.2011.01.006.

CHENG, K.L., ROAD, R. and CITY, K. (2005) On Calibration of pH Meters. pp. 209–219.

CHIU, Y.H. and LIN, L.Y. (2019) Effect of activating agents for producing activated carbon using a facile one-step synthesis with waste coffee grounds for symmetric supercapacitors. *Journal of the Taiwan Institute of Chemical Engineers*, 101, pp. 177–185, DOI:10.1016/j.jtice.2019.04.050.

CHOJNACKA, K., SAMORAJ, M., TUHY, L., MICHALAK, I., MIRONIUK, M. and MIKULEWICZ, M. (2018) Using XRF and ICP-OES in biosorption studies. *Molecules*, 23(8), DOI:10.3390/molecules23082076.

CHOWDHURY, I.R., CHOWDHURY, S., MAZUMDER, M.A.J. and AL-AHMED, A. (2022) *Removal of lead ions (Pb^{2+}) from water and wastewater: a review on the low-cost adsorbents*. Springer International Publishing.

DADA, A.O., INYINBOR, A.A., TOKULA, B.E., BELLO, O.S. and PAL, U. (2022) Preparation and characterization of rice husk activated carbon-supported zinc oxide nanocomposite (RHAC-ZnO-NC). *Heliyon*, 8(8), p. e10167. DOI:10.1016/j.heliyon.2022.e10167.

DAFFALLA, S.B., MUKHTAR, H. and SHAHARUN, M.S. (2012) Properties of activated carbon prepared from rice husk with chemical activation. *International Journal of Global Environmental Issues*, 12(2–4), pp. 107–129.

DANDAJEH ADAMU, A. and ADIE, D.B. (2020) Assessment of Lead Adsorption onto Rice Husk Activated Carbon. *Nigerian Journal of Engineering*, 27(2), pp. 2705–3954.

DANIEL RETA, Y. and DESISSA, T.D. (2023) Composites of CoFe2O4/Graphene oxide/Kaolinite for adsorption of lead ion from aqueous solution. *Frontiers in Materials*, 10(November), pp. 1–17. DOI:10.3389/fmats.2023.1277467.

DIAO, Y., WALAWENDER, W.P. and FAN, L.T. (2002) Activated carbons prepared from phosphoric acid activation of grain sorghum. *Bioresource Technology*, 81, pp. 45–52.

DIETLER, D., BABU, M., CISSE, G., HALAGE, A.A., MALAMBALA, E. and FUHRIMANN, S. (2019) Daily variation of heavy metal contamination and its potential sources along the major urban wastewater channel in Kampala, Uganda. *Environmental Monitoring and Assessment*, 191(2), DOI:10.1007/s10661-018-7175-4.

DIN, M.I., ASHRAF, S. and INTISAR, A. (2017) Comparative study of different activation treatments for the preparation of activated carbon: A mini-review. *Science Progress*, 100(3), pp. 299–312. DOI:10.3184/003685017X14967570531606.

EFOME, J.E., RANA, D., MATSUURA, T. and LAN, C.Q. (2019) Effects of operating parameters and coexisting ions on the efficiency of heavy metal ions removal by nano-fibrous metal-organic framework membrane filtration process. *Science of the Total Environment*, 674, pp. 355–362. DOI:10.1016/j.scitotenv.2019.04.187.

ELSAYED, M.A. and ZALAT, O.A. (2015) Factor Affecting Microwave Assisted Preparation of Activated Carbon from Local Raw Materials. *International Letters of Chemistry, Physics and Astronomy*, 47(February), pp. 15–23. DOI:10.18052/www.scipress.com/ILCPA.47.15.

FUTALAN, C.C., DIANA, E., EDANG, M.F.A., PADILLA, J.M., CENIA, M.C. and ALFECHE, D.M. (2023) Adsorption of Lead from Aqueous Solution Using Activated Carbon Derived from Rice Husk Modified with Lemon Juice. *Sustainability*, 15(22), p. 15955. DOI:10.3390/su152215955.

GAO, Y., YUE, Q., GAO, B. and LI, A. (2020) Insight into activated carbon from different kinds of chemical activating agents: A review. *Science of the Total Environment*, 746, p. 141094. DOI:10.1016/j.scitotenv.2020.141094.

GONZÁLEZ, P.G. (2019) Hazardous Metallic Ions Removal from Water Using Activated Carbons. *Encyclopedia of Water*, pp. 1–11. DOI:10.1002/9781119300762.wsts0097.

GUNORUBON, A.J. and CHUKWUNONSO, N. (2018) Kinetics, Equilibrium and Thermodynamics Studies of Fe^{3+} Ion Removal from Aqueous Solutions Using Periwinkle Shell Activated Carbon. *Advances in Chemical Engineering and Science*, 08(02), pp. 49–66. DOI:10.4236/aces.2018.82004.

GUO, Y., YANG, S., YU, K., ZHAO, J., WANG, Z. and XU, H. (2002) The preparation and mechanism studies of rice husk based porous carbon. *Materials Chemistry and Physics*, 74(3), pp. 320–323.

HARIMISA, G.E., JUSOH, N.W.C., TAN, L.S., SHAMELI, K., GHAFAR, N.A. and

MASUDI, A. (2022) Synthesis of potassium hydroxide-treated activated carbon via one-step activation method. *Journal of Physics: Conference Series*, 2259(1), DOI:10.1088/1742-6596/2259/1/012009.

HARUNA, A.U., MUHAMMAD, Y.A., IBRAHIM, A., MUSA, B. and NUHU, M. (2020) Effect of Activating Agents on the Production of Activated Carbon from Rice Husk. *International Journal for Scientific Research & Development*, 8(10), pp. 250–253.

HEIDARINEJAD, Z., HEIDARI, M., DEHGHANI, M.H. and ALI, I. (2020) Methods for preparation and activation of activated carbon: a review. *Environmental Chemistry Letters*, 18(2), pp. 393–415. DOI:10.1007/s10311-019-00955-0.

HUANG, Y., LI, S., LIN, H. and CHEN, J. (2014) Fabrication and characterization of mesoporous activated carbon from Lemna minor using one-step H_3PO_4 activation for Pb(II) removal. *Applied Surface Science*, 317, pp. 422–431, DOI:10.1016/j.apsusc.2014.08.152.

ZHANG, X., LIU, H., LI, Y., LI, G. and HU, C. (2015) Preparation of Activated Carbon from Pyrolytic Residue of Rice Husk and Its Application for the Adsorption of Phenol and Iodine. *Asian Journal of Chemistry*, 27(4), pp. 1513–1520. DOI:10.14233/ajchem.2015.18607.

ABAASA, N.C., AYESIGA, S., RUKUNDO, G.Z., LEJJU, J.B., BYARUGABA, F. and TAMWESIGIRE, I.K. (2023) Community perceptions and practices on quality and safety of drinking water in Mbarara city , south western Uganda. pp. 1–20. DOI:10.1371/journal.pwat.0000075.

EL JERY, A., ALAWAMLEH, H.S.K., SAMI, M.H., ABBAS, H.A., SAMMEN, S.S., AHSAN, A., IMTEAZ, M.A., SHANABLEH, A., SHAFIQUZZAMAN, M., OSMAN, H. and AL-ANSARI, N. (2024) Isotherms, kinetics and thermodynamic mechanism of methylene blue dye adsorption on synthesized activated carbon. *Scientific Reports*, 14(1), pp. 1–12. DOI:10.1038/s41598-023-50937-0.

JIANG, C., CUI, S., HAN, Q., LI, P., ZHANG, Q., SONG, J. and LI, M. (2019) Study on Application of Activated Carbon in Water Treatment. *IOP Conference Series: Earth and Environmental Science*, 237(2), DOI:10.1088/1755-1315/237/2/022049.

KAMYA, I.R., ASINGWIRE, N. and WAISWA, D.B. (2020) Besides Physical Scarcity: An Analysis of Domestic Water Access in Rural Rakai, Uganda. *Eastern Africa Social Science Research Review*, 36(2), pp. 115–131. DOI:10.1353/eas.2020.0008.

KANE, S.N., MISHRA, A. and DUTTA, A.K. (2016) The influence of activating agents on the performance of rice husk-based carbon for sodium lauryl sulfate and chrome (Cr) metal adsorptions. *Journal of Physics: Conference Series*, 755(1), DOI:10.1088/1742-6596/755/1/011001.

KAUSHAL, A. (2017) Adsorption Phenomenon and its Application in Removal of Lead from Waste Water: A Review. *International Journal of Hydrology*, 1(2), DOI:10.15406/ijh.2017.01.00008.

KHASHAN, M.H. and MOHAMMAD, A.K. (2022) Comparative study for Pb^{2+} adsorption from simulated wastewater of battery manufacture on activated carbon prepared from rice husk with different activation agents. *Al-Qadisiyah Journal for*

Engineering Sciences, 15(3), pp. 147–155, DOI:10.30772/qjes.v15i3.827.

KIM, D., HWANG, S., KIM, Y., JEONG, C.H., HONG, Y.P. and RYOO, K.S. (2019) Removal of Heavy Metals from Water Using Chicken Egg Shell Powder as a Bio-Adsorbent. *Bulletin of the Korean Chemical Society*, 40(12), pp. 1156–1161. DOI:10.1002/bkcs.11884.

KOROBOCHKIN, V. V., TU, N. V. and HIEU, N.M. (2016) Production of activated carbon from rice husk Vietnam. *IOP Conference Series: Earth and Environmental Science*, 43(1), DOI:10.1088/1755-1315/43/1/012066.

KOSHELEVA, R.I., MITROPOULOS, A.C. and KYZAS, G.Z. (2019) Synthesis of activated carbon from food waste. *Environmental Chemistry Letters*, 17(1), pp. 429–438. DOI:10.1007/s10311-018-0817-5.

LAKSHMIKANDHAN, K. and RAMADEVI, A. (2019) Removal of lead in water using activated carbon prepared from acacia catechu. *Water SA*, 45(3), pp. 374–382.

LALMI, A., BOUHIDEL, K., SAHRAOUI, B. and ANFIF, C.H. (2018) Removal of lead from polluted waters using ion exchange resin with $Ca(NO_3)_2$ for elution. *Hydrometallurgy*, 178(2017), pp. 287–293. DOI:10.1016/j.hydromet.2018.05.009

LATIFF, M.F.P.M., ABUSTAN, I., AHMAD, M.A., YAHAYA, N.K.E.M. and KHALID, A.M. (2016) Effect of preparation conditions of activated carbon prepared from corncob by CO_2 activation for removal of Cu (II) from aqueous solution. *AIP Conference Proceedings*, 1774(06), pp. 1–5. DOI:10.1063/1.4965057.

LEE, T., OOI, C., OTHMAN, R. and YEOH F. (2014) Activated carbon fiber - The hybrid of carbon fiber and activated carbon. *Reviews on Advanced Materials Science*, 36(2), pp. 118–136.

LI, Y., DING, X., GUO, Y., WANG, L., RONG, C., QU, Y., MA, X. and WANG, Z. (2011) A simple and highly effective process for the preparation of activated carbons with high surface area. *Materials Chemistry and Physics*, 127(3), pp. 495–500. DOI:10.1016/j.matchemphys.2011.02.046.

LI, Y., ZHANG, X., YANG, R., LI, G. and HU, C. (2015) The role of H3PO4 in the preparation of activated carbon from NaOH-treated rice husk residue. *RSC Advances*, 5(41), pp. 32626–32636. DOI:10.1039/c5ra04634c.

VAN LIENDEN, C., SHAN, L., RAO, S., RANIERI, E. and YOUNG, T.M. (2010) Metals Removal from Stormwater by Commercial and Non-Commercial Granular Activated Carbons. *Water Environment Research*, 82(4), pp. 351–356.

LIOU, T. and WU, S. (2009) Characteristics of microporous / mesoporous carbons prepared from rice husk under base- and acid-treated conditions. *Journal of Hazardous Materials*, 171(1-3), pp. 693–703. DOI:10.1016/j.jhazmat.2009.06.056.

LIU, Z., SUN, Y., XU, X., QU, J. and QU, B. (2020) Adsorption of Hg(II) in an Aqueous Solution by Activated Carbon Prepared from Rice Husk Using KOH Activation. *ACS Omega*, 5(45), pp. 29231–29242. DOI:10.1021/acsomega.0c03992.

LOZANO-CASTELLO, D., CALO, J.M., CAZORLA-AMOROS, D. and LINARES-SOLANO, A. (2007) Carbon activation with KOH as explored by temperature

programmed techniques, and the effects of hydrogen. *Carbon*, 45(13), pp. 2529–2536. DOI:10.1016/j.carbon.2007.08.021.

LUO, Y., LI, D., CHEN, Y., SUN, X., CAO, Q. and LIU, X. (2019) The performance of phosphoric acid in the preparation of activated carbon-containing phosphorus species from rice husk residue. *Journal of Materials Science*, 54(6), pp. 5008–5021. DOI:10.1007/s10853-018-03220-x.

ALSLAIBI, T.M., ABUSTAN, I., AHMAD, M.A. and ABU FOUL, A. (2013) A review : Production of activated carbon from agricultural byproducts via conventional and microwave heating. *Journal of Chemical Technology & Biotechnology*, 88(July 2013), pp. 1183–1190. DOI: 10.1002/jctb.04028.

MENYA, E., OLUPOT, P.W., STORZ, H., LUBWAMA, M. and KIROS, Y. (2018) Production and performance of activated carbon from rice husks for removal of natural organic matter from water: A review. *Chemical Engineering Research and Design*, 129, pp. 271–296. DOI:10.1016/j.cherd.2017.11.008.

LI, M., ZHANG, X., SU, W., CAI, F., LAN, T. and DAI, Z. (2024) Adsorption of Coxsackievirus in Sediments: Influencing Factors, Kinetics, and Isotherm Modeling. *Journal of applied sciences,* 14, 1480, DOI:10.3390/ app14041480.

MOHAMAD NOR, N., LAU, L.C., LEE, K.T. and MOHAMED, A.R. (2013) Synthesis of activated carbon from lignocellulosic biomass and its applications in air pollution control - A review. *Journal of Environmental Chemical Engineering*, 1(4), pp. 658–666, DOI:10.1016/j.jece.2013.09.017.

MOHAMMAD, Y.S., SHAIBU-IMODAGBE, E.M., IGBORO, S.B., GIWA, A. and

OKUOFU, C.A. (2015) Effect of Phosphoric Acid Modification on Characteristics of Rice Husk Activated Carbon. *Iranica Journal of energy and environment*, 6(1), pp. 20–25, DOI:10.5829/idosi.ijee.2015.06.01.05.

MORTADA, W.I., MOHAMED, R.A., ABDEL MONEM, A.A., AWAD, M.M. and HASSAN, A.F. (2023) Effective and Low-Cost Adsorption Procedure for Removing Chemical Oxygen Demand from Wastewater Using Chemically Activated Carbon Derived from Rice Husk. *Separations*, 10(1), DOI: 10.3390/separations10010043.

MUNGAI, M.J. (2015) *Optimizing conditions for preparing activated carbon from avocado seeds for best adsorption of lead ions from wastewater*. Thesis (MSc), Kenyatta University.

MUNIANDY, L., ADAM, F., MOHAMED, A.R. and POH, N. (2014) The synthesis and characterization of high purity mixed microporous/mesoporous activated carbon from rice husk using chemical activation with NaOH and KOH. *Microporous and Mesoporous Materials*, 197, pp. 316–323, DOI:10.1016/j.micromeso.2014.06.020.

NANDI, R., JHA, M.K., GUCHHAIT, S.K., SUTRADHAR, D. and YADAV, S. (2023) Impact of KOH Activation on Rice Husk Derived Porous Activated Carbon for Carbon Capture at Flue Gas alike Temperatures with High CO_2/N_2 Selectivity. *ACS Omega*, 8(5), pp. 4802–4812, DOI:10.1021/acsomega.2c06955.

OLUPOT, P.W., CANDIA, A., MENYA, E. and WALOZI, R. (2016) Characterization of rice husk varieties in Uganda for biofuels and their techno-economic feasibility in gasification. *Chemical Engineering Research and Design*, 107, pp. 63–72,

DOI:10.1016/j.cherd.2015.11.010.

ORIBAYO, O., OLALEKAN, A.P., OWOLABI, R.U., OLALEYE, O.O. and ONYEKABA, O.A. (2020) Adsorption of Cr(VI) ions from aqueous solution using rice husk–based activated carbon: Optimization, kinetic, and thermodynamic studies. *Environmental Quality Management*, 30(1), pp. 61–77, DOI:10.1002/tqem.21704.

OZDEMIR, I., SAHIN, M., ORHAN, R. and ERDEM, M. (2014) Preparation and characterization of activated carbon from grape stalk by zinc chloride activation. *Fuel Processing Technology*, 125, pp. 200–206, DOI:10.1016/j.fuproc.2014.04.002.

PARTHASARATHY, P. and NARAYANAN, S.K. (2014) Removal of Metal Impurities in Rice Husk and Characterization of Rice Husk Ash Under Simplified Acid Pretreatment Process. *Environmental Progress & Sustainable Energy*, 33(3), pp. 676–680, DOI:10.1002/ep.12513.

PRZYBYLA, A., KUC, J. and WZOREK, Z. (2022) A New Approach to the Determination of Silicon in Zinc, Lead-Bearing Materials and in Waste Using the ICP-OES Method. *Molecules*, 27(10), pp. 1–14, DOI:10.3390/molecules27103059.

RAIKAR, R. V, CORREA, S. AND GHORPADE, P. (2015) Removal of Lead (Ii) From Aqueous Solution Using Natural and Activated Rice Husk. *International Research Journal of Engineering and Technology*, 2(3), pp. 1677–1686.

REDONDO, E., CARRETERO-GONZALEZ, J., GOIKOLEA, E. and SEGALINI, J.

(2015) Effect of pore texture on performance of activated carbon supercapacitor electrodes derived from olive pits. *Electrochimica Acta*, 160, pp. 178–184, DOI:10.1016/j.electacta.2015.02.006.

REHMAN, K., FATIMA, F., WAHEED, I. and AKASH, M.S.H. (2018) Prevalence of exposure of heavy metals and their impact on health consequences. *Journal of Cellular Biochemistry*, 119(1), pp. 157–184, DOI:10.1002/jcb.26234.

SADEGHI, M., KARIMI, H. and ALIJANVAND, M.H. (2017) Removal of lead ions from industrial wastewater using precipitation process. *Environmental Engineering and Management Journal*, 16(7), pp. 1563–1568, DOI:10.30638/eemj.2017.169.

SAHIRA, J., ADHIKARI, M., POKHAREL, B.P. and PRADHANANGA, R.R. (2013) Effects of Activating Agents on the Activated Carbons Prepared from Lapsi Seed Stone. *Research Journal of Chemical Science*, 3(5), pp. 19–24.

SALAHUDEEN, N. and ALHASSAN, A. (2022) Adsorption of Crystal Violet on Rice Husk Activated Carbon. *Journal of Engineering Sciences*, 9(1), pp. F11–F15.

SERIO, M.A., KROO, E., WOJTOWICZ, M.A., SUUBERG, E.M. FILBURN, T. and et al. (2002) An Improved Pyrolyzer for Solid Waste Resource Recovery in Space. In: *Proceedings of the 32nd International Conference on Environmental Systems, San Antonio, July 15–18, 2002.* Texas: SAE Publications Group, (724).

SEVILLA, M., DIEZ, N. and FUERTES, A.B. (2021) More Sustainable Chemical Activation Strategies for the Production of Porous Carbons. *International Sustainable Chemistry Journal,* 14(1), pp. 94–117, DOI:10.1002/cssc.202001838.

SHARIFIKOLOUEI, E., BAINO, F., GALLETTI, C., FINO, D. and FERRARIS, M. (2020) Adsorption of Pb and Cd in rice husk and their immobilization in porous glass-ceramic structures. *International Journal of Applied Ceramic Technology*, 17(1), pp. 105–112, DOI:10.1111/ijac.13356.

SHARIFUL, M.I., SEPEHR, T., MEHRALI, M., ANG, B.C. and AMALINA, M.A. (2018) Adsorption capability of heavy metals by chitosan/poly(ethylene oxide)/activated carbon electrospun nanofibrous membrane. *Journal of Applied Polymer Science*, 135(7), pp. 1–14, DOI:10.1002/app.45851.

SHARMA, A., GREWAL, A.S., SHARMA, D. and SRIVASTAV, A.L. (2023) Heavy metal contamination in water: consequences on human health and environment. *Metals in Water*, pp. 39–52, DOI:10.1016/B978-0-323-95919-3.00015-X.

SINGH, K., RENU, N.A. and AGARWAL, M. (2017) Methodologies for removal of heavy metal ions from wastewater: an overview. *Interdisciplinary Environmental Review*, 18(2), p. 124.

SONG, M., WEI, Y., CAI, S., YU, L., ZHONG, Z. and JIN, B. (2018) Study on adsorption properties and mechanism of Pb^{2+} with different carbon based adsorbents. *Science of the Total Environment*, 618, pp. 1416–1422, DOI:10.1016/j.scitotenv.2017.09.268.

TAHA, M.F., CHONG, F.K., SHAHARUN, M.S. and RAMLI, A. (2011) Removal of Ni (II), Zn (II) and Pb (II) ions from Single Metal Aqueous Solution using Activated Carbon Prepared from Rice Husk. *International Journal of Enviroment, Chemical, Ecological, Geological and Geophysical Engineering*, 5(12), pp. 855–860.

TERNERO-HIDALGO, J.J., ROSAS, J.M., PALOMO, J., VALERO-ROMERO, M.J., RODRIGUEZ-MIRASOL, J. and CORDERO, T. (2016) Functionalization of activated carbons by HNO_3 treatment: Influence of phosphorus surface groups. *Carbon*, 101, pp. 409–419, DOI:10.1016/j.carbon.2016.02.015.

THITAME, P. V and SHUKLA, S.R. (2017) Removal of Lead (II) from Synthetic Solution and Industry Wastewater Using Almond Shell Activated Carbon. *Environmental Progress & Sustainable Energy*, 33(3), pp. 676–680, DOI:10.1002/ep.12616.

UYGUN, O., MURAT, A. and ÇAKAL, G.O. (2023) Magnetic sepiolite/iron(III) oxide composite for the adsorption of lead(II) ions from aqueous solutions. *Clay Minerals*, 58(3), pp. 267–279, DOI:10.1180/clm.2023.24.

LE VAN, K., THU, T.L.T., THU, H.N.T. and VAN HOANG, H. (2019) Activated Carbon by KOH and NaOH Activation: Preparation and Electrochemical Performance in K_2SO_4 and Na_2SO_4 Electrolytes. *Russian Journal of Electrochemistry*, 55(9), pp. 900–907, DOI:10.1134/S1023193519070115.

LE VAN, K. and LUONG THI THU, T. (2019) Preparation of Pore-Size Controllable Activated Carbon from Rice Husk Using Dual Activating Agent and Its Application in Supercapacitor. *Journal of Chemistry*, 2019, DOI:10.1155/2019/4329609.

UMAR, A.H., ABDULLAHI, Y.M., IBRAHIM, A., MUSA, B. and NUHU, M. (2020) Effect of Activating Agents on the Production of Activated Carbon from Rice. *International Journal for Scientific Research & Development*, 8(10/2020/051), pp. 250–253.

VIJAYARAGHAVAN, K., PALANIVELU, K. and VELAN, M. (2006) Biosorption of copper(II) and cobalt(II) from aqueous solutions by crab shell particles. *Bioresource Technology*, 97(12), pp. 1411–1419, DOI:10.1016/j.biortech.2005.07.001.

VILEN, A., LAURELL, P. and VAHALA, R. (2022) Comparative life cycle assessment of activated carbon production from various raw materials. *Journal of Environmental Management*, 324(2022), DOI:10.1016/j.jenvman.2022.116356.

VAN VLIET, M.T.H., JONES, R.R., FLORKE, M., FRANSSEN, W.H.P., HANASAKI, N., WADA, Y. and YEARSLEY, J.R. (2021) Global water scarcity including surface water quality and expansions of clean water technologies. *Environmental Research Letters*, 16(2), DOI:10.1088/1748-9326/abbfc3.

WANG, B., LAN, J., BO, C., GONG, B. and OU, J. (2023) Adsorption of heavy metal onto biomass-derived activated carbon: review. *Royal Society of Chemistry Advances*, 13(7), pp. 4275–4302, DOI:10.1039/d2ra07911a.

WANG, L., GUO, Y., ZOU, B., RONG, C., MA, X., QU, Y., LI, Y. and WANG, Z. (2011) High surface area porous carbons prepared from hydrochars by phosphoric acid activation. *Bioresource Technology*, 102(2), pp. 1947–1950, DOI:10.1016/j.biortech.2010.08.100.

WANI, A.L., ARA, A. and USMANI, J.A. (2015) Lead toxicity: A review. *Interdisciplinary Toxicology*, 8(2), pp. 55–64, DOI:10.1515/intox-2015-0009.

XIA, H., WU, J., SRINIVASAKANNAN, C., PENG, J. and ZHANG, L. (2016) Effect of Activating Agent on the Preparation of Bamboo-Based High Surface Area

Activated Carbon by Microwave Heating. *High Temperature Materials and Processes*, 35(6), pp. 535–541, DOI:10.1515/htmp-2014-0228.

YAHAYAA, N.K., MOHAMED LATIFFA, M.F.P., ABUSTANA, I. and AHMAD, M.A. (2010) Effect of preparation conditions of activated carbon prepared from rice husk by $ZnCl_2$ activation for removal of Cu (II) from aqueous solution. *International Journal of Engineering & Technology IJET-IJENS*, 10(6), pp. 2–6.

YANG, T. and LUA, A.C. (2006) Textural and chemical properties of zinc chloride activated carbons prepared from pistachio-nut shells. *Materials Chemistry and Physics*, 100(2–3), pp. 438–444, DOI:10.1016/j.matchemphys.2006.01.039.

YARKANDI, N.H. (2014) Removal of lead (II) from waste water by adsorption. *International Journal of Current Microbiology and Applied Sciences*, 3(4), pp. 207–228.

YERDAULETOV, M.S., NAZAROV, K., MUKHAMETULY, B., YELEUOV, M.A., DAULBAYEV, C., ABDULKARIMOVA, R., YSKAKOV, A., NAPOLSKIY, F. and KRIVCHENKO, V. (2023) Characterization of Activated Carbon from Rice Husk for Enhanced Energy Storage Devices. *Molecules*, 28(15), pp. 1–12, DOI:10.3390/molecules28155818.

YOUSSEF, A.M., AHMED, A.I., AMIN, M.I. and EL-BANNA, U.A. (2015) Adsorption of lead by activated carbon developed from rice husk. *Desalination and Water Treatment*, 54(6), pp. 1694–1707, DOI:10.1080/19443994.2014.896289.

YUE, Z. and ECONOMY, J. (2017) *Carbonization and activation for production of*

activated carbon fibers. United States: Elsevier Ltd.

ZAKIR, M. (2013) Adsorption of lead (II) and copper (II) ions on rice husk activated carbon under sonication 1. *International Symposium on Chemical and Bioprocess Engineering*, (June), pp. 25–28.

ZAMORA-LEDEZMA, C., NEGRETE-BOLAGAY, D., FIGUEROA, F., ZAMORA-LEDEZMA, E., NI, M., ALEXIS, F. and GUERRERO, V.H. (2021) Heavy metal water pollution: A fresh look about hazards, novel and conventional remediation methods. *Environmental Technology and Innovation*, 22, p. 101504, DOI:10.1016/j.eti.2021.101504.

APPENDICES

Table A.1: Laboratory results of the Inductively Coupled Plasma-Optical Emission Spectroscopy for ARHCK

Dosage (g/L)	Percentage concentration of KOH (w/v)				
	1.0%	2.5%	5.0%	7.5%	10.0%
	ICP-OES readings (mg/L)				
5	22.4860	1.3909	3.9330	0.3104	0.7727
10	40.2645	28.4270	11.2995	13.0340	24.9050
15	93.3285	16.4620	12.8705	13.3415	24.2990
20	143.1595	13.6260	28.4725	14.3730	89.7245
Dosage (g/L)	Percentage concentration of KOH (w/v)				
	1.0%	2.5%	5.0%	7.5%	10.0%
	Mean percentage removal (%)				
5	91.1	99.5	98.5	99.9	99.7
10	84.1	88.8	95.5	94.9	90.2
15	63.1	93.5	94.9	94.7	90.4
20	43.4	94.6	88.8	94.3	64.5

Table A.2: Laboratory results of the Inductively Coupled Plasma-Optical Emission Spectroscopy for ARHCZ

Dosage (g/L)	Percentage concentration of $ZnCl_2$ (w/v)				
	1.0%	2.5%	5.0%	7.5%	10.0%
	ICP-OES readings (mg/L)				
5	10.1320	140.5470	199.6760	129.4395	230.3570
10	8.8215	61.6295	152.2820	83.5900	172.5950
15	4.6345	48.6730	125.4150	55.6040	140.5720
20	3.7375	31.3075	44.3955	55.1055	112.4970
Dosage (g/L)	Percentage concentration of $ZnCl_2$ (w/v)				
	1.0%	2.5%	5.0%	7.5%	10.0%
	Mean percentage removal (%)				
5	96.0	44.5	21.1	48.8	9.0
10	96.5	75.6	39.8	67.0	31.8
15	98.2	80.8	50.4	78.0	44.5
20	98.5	87.6	82.5	78.2	55.5

Table A.3: Laboratory results of the Inductively Coupled Plasma-Optical Emission Spectroscopy for ARHCH

Dosage (g/L)	**Percentage concentration of H_3PO_4 (w/v)**				
	1.0%	**2.5%**	**5.0%**	**7.5%**	**10.0%**
	ICP-OES readings (mg/L)				
5	181.0130	66.2705	222.6795	170.3105	120.4140
10	121.8705	68.8535	209.7915	219.7125	112.7530
15	56.5825	49.7555	184.4270	237.5695	113.7275
20	40.3445	40.4270	166.5495	175.8070	124.7640
Dosage (g/L)	**Percentage concentration of H_3PO_4 (w/v)**				
	1.0%	**2.5%**	**5.0%**	**7.5%**	**10.0%**
	Mean percentage removal (%)				
5	28.5	73.8	12.0	32.7	52.4
10	51.8	72.8	17.1	13.2	55.4
15	77.6	80.3	27.1	6.1	55.1
20	84.0	84.1	34.2	30.5	55.7

Table A 4: Laboratory results of the Inductively Coupled Plasma-Optical Emission Spectroscopy for the inactivated RHC

Dosage (g/L)	**ICP-OES readings (mg/L)**
5	170.3671
10	155.4635
15	137.2957
20	116.7494
Dosage (g/L)	**Mean percentage removal (%)**
5	32.7
10	38.6
15	45.7
20	53.9

Table A.5: Data used for plotting Langmuir isotherm, for ARHCK

Mass of Adsorbent (mg)	Vol of soln used for Adsorption, (ml)	**C_0,** Initial Conc. (mg/l)	**C_e,** Conc. After Adsorption/Equilibrium Conc. (mg/l)	**q_e,** Pb^{2+} ions adsorbed (mg/l)	**q_e,** (mg)	**q_e,** (mg/g)
0.25	50	49.52	34.51	15.01	0.750	3001
0.25	50	81.06	65.67	15.39	0.770	3078

Mass of Adsorbent (mg)	Vol of soln used for Adsorption, (ml)	**C_0,** Initial Conc. (mg/l)	**C_e,** Conc. After Adsorption/Equilibrium Conc. (mg/l)	**q_e,** Pb^{2+} ions adsorbed (mg/l)	**q_e,** (mg)	**q_e,** (mg/g)
0.25	50	120.31	105.56	14.75	0.738	2951
0.25	50	161.04	146.27	14.77	0.738	2954
0.25	50	201.25	186.67	14.58	0.729	2917
0.25	50	250.64	234.72	15.92	0.796	3184

Langmuir isotherm	
C_e (mg/L)	**C_e/q_e (g/L)**
34.512	0.011
65.666	0.021
105.557	0.036
146.274	0.050
186.666	0.064
234.717	0.074

Table A.6: Data used for plotting Langmuir isotherm, for ARHCZ

Mass of Adsorbent (mg)	Vol of soln used for Adsorption, (ml)	**C_0,** Initial Conc. (mg/l)	**C_e,** Conc. After Adsorption/Equilibrium Conc. (mg/l)	**q_e,** Pb^{2+} ions adsorbed (mg/l)	**q_e,** (mg)	**q_e,** (mg/g)
0.25	50	49.52	36.73	12.79	0.640	2558
0.25	50	81.06	67.88	13.18	0.659	2635
0.25	50	120.31	107.77	12.54	0.627	2507
0.25	50	161.04	148.49	12.55	0.628	2511
0.25	50	201.25	188.88	12.37	0.618	2474
0.25	50	250.64	236.93	13.71	0.685	2741

Langmuir isotherm	
C_e (mg/L)	**C_e/q_e (g/L)**
36.728	0.014
67.881	0.026
107.773	0.043
148.489	0.059
188.881	0.076
236.932	0.086

Table A.7: Data used for plotting Langmuir isotherm, for ARHCH

Mass of Adsorbent (mg)	Vol of soln used for Adsorption, (ml)	**C_0,** Initial Conc. (mg/l)	**C_e,** Conc. After Adsorption/Equilibrium Conc. (mg/l)	**q_e,** Pb^{2+} ions adsorbed (mg/l)	**q_e,** (mg)	**q_e,** (mg/g)
0.25	50	49.52	38.50	11.02	0.551	2204
0.25	50	81.06	69.65	11.41	0.570	2281
0.25	50	120.31	109.54	10.77	0.538	2154
0.25	50	161.04	150.26	10.79	0.539	2157
0.25	50	201.25	190.65	10.60	0.530	2120
0.25	50	250.64	238.70	11.94	0.597	2388

Langmuir isotherm	
C_e (mg/L)	**C_e/q_e (g/L)**
38.497	0.017
69.650	0.031
109.542	0.051
150.258	0.070
190.651	0.090
238.702	0.100

Research photographs

Putting the RHC in oven

Checking on the RHC during drying

Grinding the RHC in blender

Storing ARHC in air-tight polythene bags

Weighing the adsorbent

Filtering the solution of Pb^{2+} mixed with adsorbent

Potassium hydroxide pellets

15ml of filtrate transferred into falcon tubes

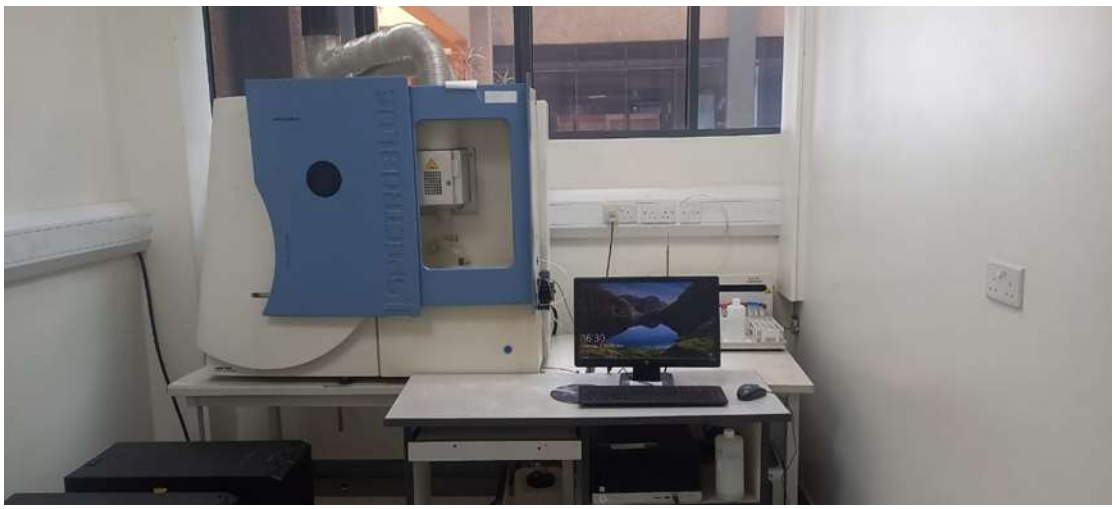

The inductively coupled plasma-optical emission spectroscopy